Multiple N−H Bond Activation: Synthesis and Reactivity of Functionalized Primary Amido Ytterbium Complexes

Chengfu Pi,[†] Zhengxing Zhang,[†] Zhen Pang,[†] Jie Zhang,[†] Jun Luo,[†] Zhenxia Chen,[†] Linhong Weng,[†] and Xigeng Zhou*[,†,‡]

Department of Chemistry, Molecular Catalysis and Innovative Material Laboratory, Fudan University, Shanghai 200433, People's Republic of China, and State Key Laboratory of Organometallic Chemistry, Shanghai 200032, People's Republic of China

Received December 1, 2006

A series of new functionalized amido complexes of ytterbium, $[Cp_2YbNHR]_2$ (R = 8-quinolyl(Qu) (**1a**), 2-pyridyl(Py) (**1b**), 2-aminophenyl (**1c**), 3-amino-2-pyridyl (**1d**), and $Cp_2Yb[NHC_6H_4(CH_2NH_2\text{-}2)]$ (**1e**), have been synthesized by metathesis of Cp_2YbCl and the corresponding amido lithium salts. Their reactivity toward carbodiimides has been investigated, in which multiple N−H activation behavior for metal-bound neutral NH_2 and anionic nitrogen-containing fragments, a property that is expressed without dissociation from the lanthanide center, is observed. These results provide an alternative mechanistic insight for the metal-mediated mono- and diguanylation of primary amines and elucidate factors that affect the chemo- and regioselectivities of the addition and protonation steps. Reaction of **1a** with 2 equiv of RN═C═NR [R = cyclohexyl (Cy), isopropyl (^{i}Pr)] leads to the formal insertion of carbodiimide into the N−H bond of the Yb-bonded amido group to yield $Cp_2Yb[\eta^1{:}\eta^2\text{-}RNC(NHR)NQu]_2$ [R = Cy (**2a**), ^{i}Pr (**2b**)]. Interestingly, treatment of **1b** with RN═C═NR affords the unexpected products $(Cp_2Yb)_2[\mu\text{-}\eta^2{:}\eta^2\text{-}PyNC(NR)_2](THF)$ [R = Cy (**3a**), ^{i}Pr (**3b**)], representing the first example of dianionic guanidinate lanthanide complexes. The reaction of **1c** with 2 equiv of RN═C═NR in THF at room temperature leads to the isolation of the single N−H addition products $Cp_2Yb[\eta^1{:}\eta^2\text{-}RNC(NHR)NC_6H_4\text{-}NH_2\text{-}2]$ [R = Cy (**4a**), ^{i}Pr (**4b**)] in satisfied yields, while treatment of **1c** with 4 equiv of RN═C═NR under the same conditions gives the double N−H addition products $Cp_2Yb[\eta^1{:}\eta^2\text{-}RNC(NHR)NC_6H_4\text{-}\{NC(NHR)_2\text{-}2\}]$ [R = Cy (**5a**), ^{i}Pr (**5b**)], via the intraligand proton transfer from chelating NH_2 to the guanidinate group of **4** to give new amido intermediates, followed by a second RN═C═NR insertion into the N−H bond of the resulting amido groups. Complexes **5** can also be obtained by reacting **4** with 1 equiv of RN═C═NR. The double-addition product $Cp_2Yb[\eta^1{:}\eta^2\text{-}CyNC(NHCy)NC_5H_3N\{NC(NHCy)_2\text{-}3\}]$ (**6**) could be obtained as red crystals from the 1:4 reaction between **1d** and CyN═C═NCy in 63% yield. Interestingly, **6** can be converted into $(Cp_2Yb)_2[\eta^2{:}\eta^3\text{-}(CyN)_2CNC_5H_3N\{NC(NHCy)_2\text{-}3\}]$ (**7**) under reflux in THF and with liberation of a neutral diguanidine, $C_5H_3N(NC(NHCy)_2)\text{-}2,3$. A preference of the proton transfer to the second carbodiimide insertion into the N−H bond in the formation of **5** and **6** has been confirmed by the fact that treatment of weaker acidic **1e** with an excess of carbodiimides in THF/toluene, even with prolonged heating, provides only the monoaddition product $Cp_2Yb[\eta^2{:}\eta^1\text{-}CyNC(NHCy)\text{-}NC_6H_4(CH_2NH_2\text{-}2)]$ [R = Cy (**8a**), ^{i}Pr (**8b**)]. All complexes were characterized by elemental analysis and spectroscopic properties. The structures of all complexes except **2b**, **3b**, **4a**, and **5b** were also determined through X-ray crystal diffraction analysis.

Introduction

Amido complexes have been employed as intermediates in many catalytic reactions.[1] To develop the diverse application of amido complexes in organic transformations and to elucidate the mechanism of some important ones and thereby design a more ideal catalyst, significant efforts have focused on a detailed understanding of the nature and chemical behavior of lanthanide amido complexes over the last decade.[2−4] Noticeably, in contrast to the considerable literature available on reactivity of amido lanthanide complexes,[3] less is known about the effect of the chelating interaction on insertions into the lanthanide−nitrogen bonds.[4] Given the fact that organolanthanide can promote the intramolecular hydroamination of unsaturated amines,[1a,5] we are interested in contributing to this field by exploring unique reactivities based on other functionalized amido ligands, especially the neighboring NH_2 group participating in the interaction when complexed to the lanthanide metals.

Recently, we have found that the reactivity behavior of amido lanthanide complexes is often dependent on the nature of the amido ligands. For example, the reactivities of primary amido

* Corresponding author. E-mail: xgzhou@fudan.edu.cn.
† Fudan University.
‡ State Key Laboratory of Organometallic Chemistry, Shanghai.

(1) (a) Hong, S.; Marks, T. J. *Acc. Chem. Res.* **2004**, *37*, 673. (b) Muller, T. E.; Beller, M. *Chem. Rev.* **1998**, *98*, 675. (c) Muller, T. E.; Grosche, M.; Herdtweck, E.; Pleier, A. K.; Walter, E.; Yan, Y. K. *Organometallics* **2000**, *19*, 170.

(2) (a) Yao, Y. M.; Zhang, Z. Q.; Peng, H. M.; Zhang, Y.; Shen, Q.; Lin, J. *Inorg. Chem.* **2006**, *45*, 2175. (b) Tobisch, S. *Chem.−Eur. J.* **2005**, *11*, 6372. (c) Collin, J.; Daran, J. C.; Jacquet, O.; Schulz, E.; Trifonov, A. *Chem.−Eur. J.* **2005**, *11*, 3455. (d) Scott, N. M.; Kempe, R. *Eur. J. Inorg. Chem.* **2005**, *7*, 1319. (e) Schuetz, S. A.; Silvernail, C. M.; Incarvito, C. D.; Rheingold, A. L.; Clark, J. L.; Day, V. W.; Belot, J. A. *Inorg. Chem.* **2004**, *43*, 6203.

10.1021/om061094+ CCC: $37.00
Publication on Web 03/13/2007

Scheme 1

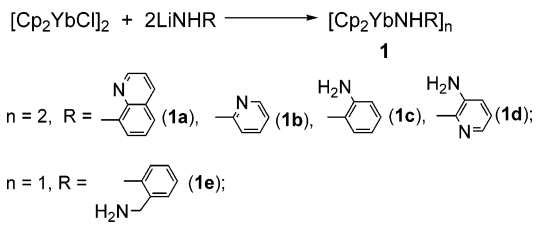

lanthanide complexes toward carbodiimides and ketenes are markedly different from those of the secondary amido complexes.[6] However, the question of whether initial addition mode (Ln−N or N−H addition) or subsequent isomerization plays a key role in determining these differences is still an open issue. It is known that the chelating effect disfavors ligand dissociation and, thus, retards frequently the insertion of unsaturated substrates into the metal−ligand bond.[7] Therefore, it would be expected that the N−H addition could be distinguished from the Ln−N addition if the presence of chelating substituents could prevent migration of the amido in an effective carbodiimide reaction process.

On the other hand, carbon−nitrogen bond-forming reactions are important fundamental transformations in synthetic chemistry. Catalytic hydroamination of unsaturated carbon−carbon and carbon−nitrogen functionalities has proven to be a straightforward and atom-economical route to nitrogen-containing compounds in organic chemistry. Catalysts based on rare-earth metals have been proven to be particularly active for these kinds of reactions.[1a,5a,8] Although such transformations appear to proceed through transformation of amines into the stronger nucleophilic amides by deprotonation and subsequent nucleophilic addition to a C−C or C−N multiple bond, structural information on their intermediates is still considerably limited.[1a,8] Our long-term interest in the reactivity of lanthanide amido complexes[6,9] and activation of the NH_2[10] group gave us a particular impetus to combine these two areas to assess the structural and chemical implications of species that encompass both. In this case it would be expected that such mixed amino/amido lanthanide complexes would display new and interesting patterns of reactivity compared to their individual counterparts. In addition, if an intraligand proton transfer reaction from amino to the resulting guanidinate group can take place when lanthanide complexes containing the mixed amino−amido ligand are reacted with carbodiimides, this would allow the isolation of unusual metal complexes showing unique bonding or patterns of reactivity and provide insight into the complete organolanthanide-catalyzed guanylation reaction course. Herein, we present a detailed study of the synthesis and carbodiimide insertion of a series of ytterbocene complexes featuring different functionalized primary amido ligands, demonstrating that the chelating effect and neighboring NH_2 substituent participation interaction can impart to lanthanide amides an enhanced reactivity and representing the first dianionic guanidinate lanthanide complexes.

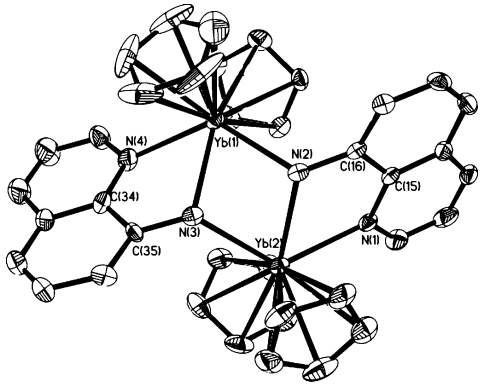

Figure 1. Thermal ellipsoid (30%) plot of complex **1a**. Hydrogen atoms are omitted for clarity. Key bond lengths (Å) and angles (deg): Yb(1)−N(3) 2.387(6), Yb(1)−N(2) 2.439(6), Yb(1)−N(4) 2.484(7), Yb(2)−N(1) 2.488(6), Yb(2)−N(2) 2.383(5), Yb(2)−N(3) 2.424(6), N(2)−C(16) 1.401(9), N(3)−C(35) 1.376(9), N(1)−C(15) 1.379(9), N(4)−C(34) 1.364(10), N(3)−Yb(1)−N(2) 64.7(2), N(2)−Yb(2)−N(3) 65.0(2), Yb(1)−N(3)−Yb(2) 100.6(2), Yb(2)−N(2)−Yb(1) 100.3(2), N(2)−Yb(2)−N(1) 67.16(19), N(3)−Yb(1)−N(4) 67.4(2).

Results and Discussion

Synthesis and Structure of Ytterbium Amido Complexes. The reaction of 2 equiv of lithium 8-quinolylamido (QuNHLi) with $[Cp_2YbCl]_2$ affords a red crystalline product, **1a**, in 59% yield. Using a similar protocol to the synthesis of **1a**, the lithiation of the corresponding aromatic amines followed by an addition of a toluene solution of $[Cp_2YbCl]_2$ at low temperature results in the formation of **1b**−**e** in moderate yields (Scheme 1).

The ytterbium amido complexes described in this paper are all orange to red crystalline solids, which are extremely air- and moisture-sensitive, readily dissolving in aromatic solvents such as benzene and toluene as well as in coordinating solvents (e.g., THF, pyridine). Complexes **1a**−**e** are thermally stable at room temperature and can be stored indefinitely under an inert atmosphere. Confirmation of the empirical units of **1a**−**e** was obtained by elemental analysis and spectroscopic methods. In

(3) (a) Evans, W. J.; Ansari, M. A.; Ziller, J. W. *Inorg. Chem*. **1996**, *35*, 5435. (b) Chan, H. S.; Li, H. W.; Xie, Z. *Chem. Commun.* **2002**, 652. (c) Gordon, J. C.; Giesbrecht, G. R.; Clark, D. L.; Hay, P. J.; Keogh, D. W.; Poli, R.; Scott, B. L.; Watkin, J. G. *Organometallics* **2002**, *21*, 4726. (d) Giesbrecht, G. R.; Collis, G. E.; Gordon, J. C.; Clark, D. L.; Scott, B. L.; Hardman, N. J. *J. Organomet. Chem.* **2004**, *689*, 2177. (e) Giesbrecht, G. R.; Gordon, J. C.; Clark, D. L.; Hay, P. J.; Scott, B. L.; Tait, C. D. *J. Am. Chem. Soc.* **2004**, *126*, 6387. (f) Knight, L. K.; Piers, W. E.; Fleurat-Lessard, P.; Parvez, M.; McDonald, R. *Organometallics* **2004**, *23*, 2087. (g) Cui, C.; Shafir, A.; Schmidt, J. A. R.; Oliver, A. G.; Arnold, J. *Dalton Trans.* **2005**, 1387. (h) O'Connor, P. E.; Twamley, B.; Berg, D. J. *Inorg. Chim. Acta* **2006**, *359*, 2870. (i) Layfield, R. A.; Bashall, A.; McPartlin, M.; Rawson, J. M.; Wright, D. S. *Dalton Trans.* **2006**, 1660.

(4) (a) Zhou, X. G.; Ma, H. Z.; Huang, X. Y.; You, X. Z. *J. Chem. Soc., Chem. Commun.* **1995**, 2483. (b) Zhou, X. G.; Huang, Z. E.; Cai, R. F.; Zhang, L. B.; Zhang, L. X.; Huang, X. Y. *Organometallics* **1999**, *18*, 4128. (c) Zhou, X. G.; Ma, W. W.; Huang, Z. E.; Cai, R. F.; You, X. Z.; Huang, X. Y. *J. Organomet. Chem.* **1997**, *309*, 545. (d) Zhang, J.; Cai, R. F.,; Weng, L. H.; Zhou, X. G. *Organometallics* **2003**, *22*, 5385. (e) Evans, W. J.; Fujimoto, C. H.; Ziller, J. W. *Organometallics* **2001**, *20*, 4529.

(5) (a) Molander, G. A.; Romero, J. A. C. *Chem. Rev.* **2002**, *102*, 2161, and references therein. (b) Hong, S. W.; Kawaoka, A. M.; Marks, T. J. *J. Am. Chem. Soc.* **2003**, *125*, 15878. (c) Hong, S. W.; Tian, S.; Metz, M. V.; Marks, T. J. *J. Am. Chem. Soc.* **2003**, *125*, 14768. (d) Molander, G. A.; Pack, S. K. *J. Org. Chem.* **2003**, *68*, 9214. (e) Gribkov, D. V.; Hultzsch, K. C.; Hampell, F. *Chem.−Eur. J.* **2003**, *9*, 4796. (f) Hultzsch, K. C.; Hampel, F.; Wagner, T. *Organometallics* **2004**, *23*, 2601.

(6) (a) Liu, R. T.; Zhang, C. M.; Zhu, Z. Y.; Luo, J.; Zhou, X. G.; Weng, L. H. *Chem.−Eur. J.* **2006**, *12*, 6940. (b) Zhang, J.; Cai, R. F.; Weng, L. H.; Zhou, X. G. *Organometallics* **2004**, *23*, 3303.

(7) (a) Zhang, J.; Cai, R. F.; Weng, L. H.; Zhou, X. G. *Organometallics* **2003**, *22*, 5385. (b) Zhang, W. X.; Nishiura, M.; Hou, Z. M. *J. Am. Chem. Soc.* **2005**, *127*, 16788.

(8) Zhang, W. X.; Nishiura, M.; Hou, Z. M. *Synlett* **2006**, 1213.

(9) Zhang, J.; Cai, R. F.; Weng, L. H.; Zhou, X. G. *J. Organomet. Chem.* **2003**, *672*, 94.

(10) (a) Ma, L. P.; Zhang, J.; Zhang, Z. X.; Cai, R. F.; Chen, Z. X.; Zhou, X. G. *Organometallics* **2006**, *25*, 4571. (b) Zhang, J.; Ma, L.; Cai, R. F.; Weng, L. H.; Zhou, X. G. *Organometallics* **2005**, *24*, 738. (c) Zhang, J.; Cai, R. F.; Weng, L. H.; Zhou, X. G. *Dalton Trans*. **2006**, 1168.

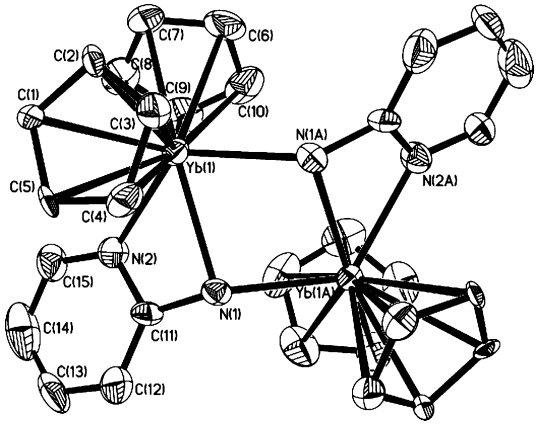

Figure 2. Thermal ellipsoid (30%) plot of complex **1b**. Hydrogen atoms are omitted for clarity. Key bond lengths (Å) and angles (deg): Yb(1)−N(1) 2.472(13), Yb(1)-N(1A) 2.369(12), Yb(1)−N(2) 2.390(6), C(11)−N(1) 1.39(2), N(2)−C(15) 1.36(3), N(2)−C(11) 1.36(3), N(1A)−Yb(1)−N(2) 123.9(3), Yb(1A)−N(1)−Yb(1) 100.4(4), N(2)−Yb(1)−N(1) 55.6(3), C(11)−N(2)−Yb(1) 97.7(2), N(2)−C(11)−N(1) 111.0(6), C(11)−N(1)−Yb(1) 92.3(7).

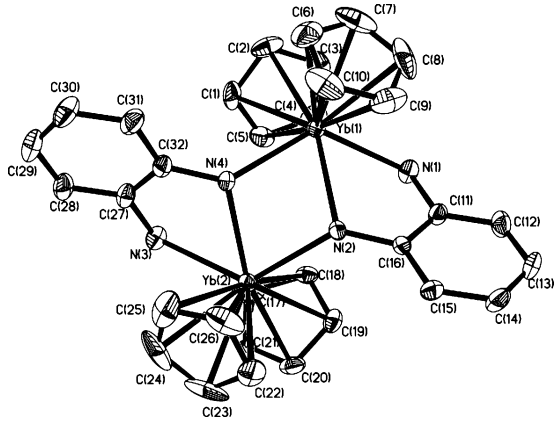

Figure 3. Thermal ellipsoid (30%) plot of complex **1c**. Hydrogen atoms are omitted for clarity. Key bond lengths (Å) and angles (deg): Yb(1)−N(4) 2.398(5), Yb(1)−N(2) 2.411(5), Yb(1)−N(1) 2.481(5), Yb(2)−N(4) 2.388(5), Yb(2)−N(2) 2.412(5), Yb(2)−N(3) 2.502(5), N(1)−C(11) 1.438(7), N(2)−C(16) 1.409(7), N(3)−C(27) 1.446(7), N(4)−C(32) 1.406(7), N(4)−Yb(1)−N(2) 66.2(2), Yb(1)−N(2)−Yb(2) 101.3(2), Yb(2)−N(4)−Yb(1) 102.4(2), N(4)−Yb(2)−N(2) 66.3(2).

the IR spectral data, all complexes show sharp N−H stretching vibrations of coordinated amido groups in the range 3200−3500 cm^{-1}, in addition to absorptions due to the Cp and aromatic functional groups. However, examination of compounds **1a**−**e** by ^1H NMR spectroscopy was hampered by their paramagnetism. To establish the solid-state molecular structures of **1a**−**e**, single-crystal X-ray analyses were undertaken, and the results are presented in Figures 1−5, respectively. Complete details of the structural analyses of these compounds are listed in Table 1 and 2. The X-ray diffraction analyses indicate that complexes **1a**−**d** are dimeric structures, while **1e** is a monomeric structure.

Each of the dimers **1a**−**d** contains two Yb^{3+} ions bridged by two aromatic amido ligands to result in butterfly-like $[Yb_2N_2]$ cores. Each Yb^{3+} ion is bonded to two anionic NH centers and one neutral donor N atom and is additionally bonded to two terminal η^5-Cp groups. Overall, this bonding arrangement results in a formal coordination number of nine for each Yb^{3+} center (Figures 1−4). Although the nitrogen-containing ligand has been deprotonated and acts as both a η^2-*N*,*N*′ chelating and a μ-bridging ligand in each of complexes **1a**−**d**, there are different

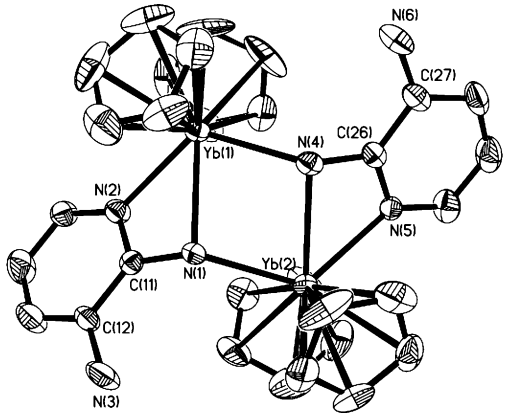

Figure 4. Thermal ellipsoid (30%) plot of complex **1d**. Hydrogen atoms are omitted for clarity. Key bond lengths (Å) and angles (deg): Yb(1)−N(4) 2.361(6), Yb(1)−N(2) 2.412(7), Yb(1)−N(1) 2.474(7), Yb(2)−N(1) 2.342(6), Yb(2)−N(5) 2.409(7), Yb(2)−N(4) 2.465(7), N(3)−C(12) 1.405(11), N(6)−C(27) 1.382(12), N(4)−C(26) 1.398(10), N(1)−C(11) 1.375(9), N(2)−C(11) 1.345(10), N(5)−C(26) 1.350(10), N(2)−C(11)−N(1) 111.9(7), N(5)−C(26)−N(4) 112.2(7), N(2)−Yb(1)−N(1) 55.0(2), N(5)−Yb(2)−N(4) 55.8-(2), N(4)−Yb(1)−N(1) 71.4(2), N(1)−Yb(2)−N(4) 71.8(2), Yb-(2)−N(1)−Yb(1) 101.0(2), Yb(1)−N(4)−Yb(2) 100.7(2).

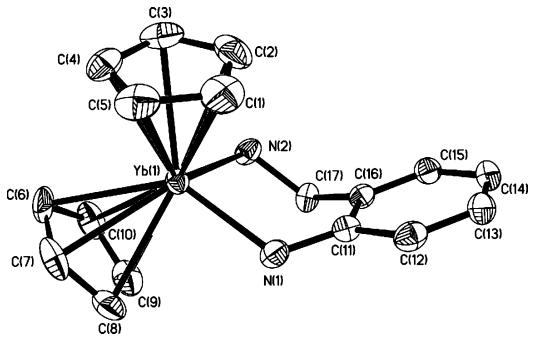

Figure 5. Thermal ellipsoid (30%) plot of complex **1e**. Hydrogen atoms are omitted for clarity. Key bond lengths (Å) and angles (deg): Yb(1)−N(1) 2.220(5), Yb(1)−N(2) 2.395(5), C(11)−N(1) 1.374(7), C(17)−N(2) 1.491(7), N(1)−Yb(1)−N(2) 84.5(2).

Scheme 2

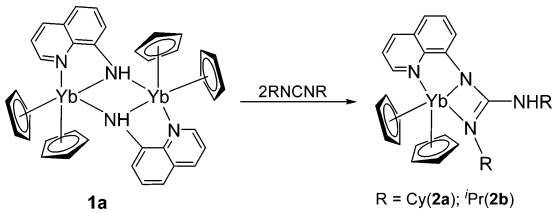

1a R = Cy(**2a**); ^{i}Pr(**2b**)

distinctive metal−nitrogen distances. The flexibility of both the bridging amido and the chelating nitrogen ytterbium distances may attest to a sensitivity of the binding situation depending on the functional substituents at the amido nitrogen. The mean Ln−N distances in the puckered $[Yb_2N_2]$ cores are 2.43, 2.42, 2.40, and 2.41 Å for **1a**−**d**, respectively, and fall in the normal ranges of Ln−N(bridging) bonds.[3h,11] Within the core of these dimers, it is noticeable that the N−Yb−N angles are distinctly acute and fall within a very broad range of 55.6(3)−66.3(2)°, whereas the Yb−N−Yb angles are somewhat narrower and lie within a range of 99.9(5)−102.4(2)°. In addition, for **1b** and **1d** a delocalization of ytterbium−nitrogen bonds as in the case

(11) Gröb, T.; Seybert, G.; Massa, W.; Weller, F.; Palaniswami, R.; Greiner, A.; Dehnicke, K. *Angew. Chem., Int. Ed.* **2000**, *39*, 4373.

Table 1. Crystal and Data Collection Parameters of Complexes 1a, 1b, 1c, and 1d

	1a	1b	1c	1d
formula	$C_{38}H_{34}N_4Yb_2$	$C_{30}H_{30}N_4Yb_2$	$C_{32}H_{34}N_4Yb_2$	$C_{30}H_{32}N_6Yb_2$
molecular weight	892.77	792.66	820.72	822.70
cryst color	orange-red	red	orange	orange
cryst dimens (mm)	0.15 × 0.10 × 0.10	0.20 × 0.18 × 0.15	0.20 × 0.15 × 0.10	0.15 × 0.10 × 0.10
cryst syst	monoclinic	orthorhombic	monoclinic	monoclinic
space group	*P*2(1)/*c*	*Fdd*2	*P*2(1)/*c*	*P*2(1)/*c*
unit cell dimens				
a (Å)	11.191(4)	40.03(2)	13.409(4)	19.693(7)
b (Å)	15.599(5)	10.439(6)	10.221(3)	18.826(6)
c (Å)	36.782(11)	13.111(8)	21.136(7)	16.666(6)
β (deg)	94.926(5)	90	97.111(5)	113.394(4)
V (Å$^{3)}$	6397(3)	5479(5)	2874.3(16)	5671(3)
Z	8	8	4	8
D_c (g·cm^{-3})	1.854	1.922	1.897	1.927
μ (mm^{-1})	5.845	6.810	6.494	6.585
F(000)	3440	3024	1576	3152
radiation (λ = 0.710730Å)	Mo Kα	Mo Kα	Mo Kα	Mo Kα
temperature (K)	293(2)	293(2)	293(2)	293(2)
scan type	$\phi-\omega$	$\phi-\omega$	$\phi-\omega$	$\phi-\omega$
θ range (deg)	1.42 to 25.01	2.03 to 25.00	1.53 to 26.01	1.56 to 26.01
h,*k*,*l* range	$-13 \le h \le 13$, $-17 \le k \le 18$, $-43 \le l \le 38$	$-47 \le h \le 29$, $-11 \le k \le 12$, $-15 \le l \le 15$	$-16 \le h \le 14$, $-12 \le k \le 12$, $-26 \le l \le 24$	$-24 \le h \le 22$, $-23 \le k \le 20$, $-20 \le l \le 17$
no. of reflns measd	26 387	5557	12 887	15 088
no. of unique reflns	11 261 [R_{int} = 0.0549]	2372 [R_{int} = 0.0856]	5613 [R_{int} = 0.0573]	11 119 [R_{int} = 0.0707]
completeness to θ	99.8% (θ = 25.01)	100.0% (θ = 25.00)	99.2% (θ = 26.01)	99.7% (θ = 26.01)
max. and min. transmn	0.5926 and 0.4743	0.4282 and 0.3429	0.5628 and 0.3566	0.7681 and 0.6058
refinement method	full-matrix least-squares on F^2	full-matrix least-squares on F^2	full-matrix least-squares on F^2	full-matrix least-squares on F^2
no. of data/restraints/params	1261/0/793	2372/61/160	5613/0/351	11 119/0/685
goodness-of-fit on F^2	0.949	1.027	0.937	0.875
final *R* indices [$I > 2\sigma(I)$]	R_1 = 0.0422, wR_2 = 0.0678	R_1 = 0.0551, wR_2 = 0.1343	R_1 = 0.0325, wR_2 = 0.0617	R_1 = 0.0431, wR_2 = 0.0839
R indices (all data)	R_1 = 0.0714, wR_2 = 0.0743	R_1 = 0.0598, wR_2 = 0.1364	R_1 = 0.0435, wR_2 = 0.0645	R_1 = 0.0732, wR_2 = 0.0934
largest diff peak and hole (e·Å^{-3})	0.995 and −1.168	2.632 and −1.293	1.124 and −1.118	1.443 and −2.530

of the amidinato ligand system takes place for pyridylamido ligands.[12] The $N_{Py}-C-N_{amido}$ angles of 111(1)° (**1b**) and 112(1)° (**1d**) instead of the desired 120° verify the strained bonding mode.

As expected, for complex **1e** (Figure 5) the Yb(1)−N(1) bond distance, 2.220(5) Å, is shorter than the average Yb−N(bridging) distances observed in **1a**−**d** and similar to the value found in $Yb(NHC_6H_3{}^iPr_2\text{-}2,6)_3(THF)_2$ (average 2.17 Å).[13] The Yb(1)−N(2) distance of 2.395(5) Å is also much shorter than the related distances of 2.481(5) and 2.502(5) Å in **1c**.

Reactivity of [Cp$_2$Yb(μ-η^2:η^1-NHQu)]$_2$ (1a) toward Carbodiimides. As illustrated in Scheme 2, **1a** reacted with 2 equiv of carbodiimides in THF to give the products from formal carbodiimide insertion into the N−H bond, $Cp_2Yb[\eta^1{:}\eta^2\text{-}RNC(NHR)NQu]_2$ [R = Cy (**2a**), ^{i}Pr (**2b**)], as determined by X-ray crystal analysis.

The molecular structure of **2a** (Figure 6) exemplifies the coordinative dexterity of the new ligand system. The structure of **2a** confirms that insertion into the N−H bond was preferred to insertion into the Ln−N bond.[14] **2a** is a solvent-free monomer with the Yb atom bonded to two η^5-cyclopentadienyl rings and three nitrogen atoms of the quinolyl-substituted guanidinate ligand to form an edge-bridged tetrahedral geometry. The coordination number of the central Yb^{3+} is nine. As expected, the coordinated guanidinate group forms essentially a planar four-membered ring with the lanthanide metal within experimental error. The bond angles around C(20) are consistent with sp^2 hybridization. Characteristically, the C(20)−N(2) and C(20)−N(3) distances of the guanidinate group are approximately equivalent and significantly longer than the C(20)−N(4) distance, indicating that the former has "single-bond" character and the latter has double-bond character.[15] Consistent with this observation, the Yb−N(2) distance of 2.265(3) Å is similar to the average values observed for the Yb−N single-bond distances in $Cp_2Yb[PhNC(NH^iPr)N^iPr]$ (2.254 Å),[6b] whereas the Yb−N(4) distance of 2.447(3) Å is comparable to the Yb−N donor bond distance in **1c**. However, in previously reported lanthanide guanidinate complexes the π-electrons of the C=N double bond are delocalized over the N−C−N unit.[9,16] This difference might be attributed to the chelating effect of the quinolyl ring.

Reactivity of [Cp$_2$Yb(μ-η^2:η^1-NHPy)]$_2$ (1b) toward Carbodiimides. Pyridylamido ligands are an important class of amido ligands and can coordinate a variety of metal complexes in the strained η^2-fashion.[17] Primary investigation results show that this binding mode can initiate a special reactivity. For example, lanthanide pyridylamido ate complexes are efficient catalysts for the ring-opening polymerization of ϵ-caprolactone and δ-valerolactone,[18] while Ni(II) pyridylamido complexes can

(12) Zhang, J.; Ruan, R. Y.; Shao, Z. H.; Cai, R. F.; Weng, L. H.; Zhou, X. G. *Organometallics* **2002**, *21*, 1420.

(13) Evans, W. J.; Ansari, M. A.; Ziller, J. W. *Inorg. Chem.* **1996**, *35*, 5435.

(14) (a) Holland, A. W.; Bergman, R. G. *J. Am. Chem. Soc.* **2002**, *124*, 14684. (b) Rais, D.; Bergman, R. G. *Chem.−Eur. J.* **2004**, *10*, 3970.

(15) Allen, F. H.; Kennard, O.; Watson, D. G.; Brammer, L.; Orpen, A. G. *J. Chem. Soc., Perkin Trans. 2* **1987**, S1.

(16) (a) Luo, Y. J.; Yao, Y. M.; Shen, Q.; Yu, K. B.; Weng, L. H. *Eur. J. Inorg. Chem.* **2003**, 318. (b) Yao, Y. M.; Luo, Y. J.; Chen, J. L.; Zhang, Z. Q.; Zhang, Y.; Shen, Q. *J. Organomet. Chem.* **2003**, *679*, 229. (c) Trifonov, A. A.; Lyubov, D. M.; Fukin, G. K.; Baranov, E. V.; Kurskii, Y. A. *Organometallics* **2006**, *25*, 3935. (d) Trifonov, A. A.; Skvortsov, G. G.; Lyubov, D. M.; Skorodumova, N. A.; Fukin, G. K.; Baranov, E. V.; Glushakova, V. N. *Chem.−Eur. J.* **2006**, *12*, 5320.

Table 2. Crystal and Data Collection Parameters of Complexes 1e, 2a, and 3a

	1e	2a	3a
formula	$C_{17}H_{19}N_2Yb$	$C_{32}H_{39}N_4Yb$	$C_{42}H_{54}N_4OYb_2$
molecular weight	424.38	652.71	976.97
cryst color	red	orange-red	bright yellow
cryst dimens (mm)	0.20 × 0.10 × 0.05	0.15 × 0.12 × 0.10	0.20 × 0.10 × 0.10
cryst syst	orthorhombic	tetragonal	orthorhombic
space group	*P*2(1)2(1)2(1)	$I\bar{4}$	*Iba*2
unit cell dimens			
a (Å)	8.743(3)	23.396(5)	20.310(6)
b (Å)	11.184(3)	23.396(5)	42.705(12)
c (Å)	15.741(5)	10.755(4)	9.543(3)
β (deg)	90	90	90
V (Å$^{3)}$	1539.1(8)	5887(3)	8278(4)
Z	4	8	8
D_c (g·cm^{-3})	1.831	1.473	1.568
μ (mm^{-1})	6.067	3.203	4.526
F(000)	820	2632	3856
radiation (λ =0.710730 Å)	Mo Kα	Mo Kα	Mo Kα
temperature (K)	293(2)	293(2)	293(2)
scan type	$\phi-\omega$	$\phi-\omega$	$\phi-\omega$
θ range (deg)	2.23 to 26.00	1.74 to 27.01	0.95 to 25.01
h,k,l range	$-10 \le h \le 10$, $-13 \le k \le 13$, $-13 \le l \le 19$	$-29 \le h \le 29$, $-17 \le k \le 29$, $-13 \le l \le 13$	$-24 \le h \le 24$, $-50 \le k \le 41$, $-11 \le l \le 11$
no. of reflns measd	7041	14 683	17 105
no. of unique reflns	2983 [R_{int} = 0.0331]	6350 [R_{int} = 0.0394]	7182 [R_{int} = 0.0384]
completeness to θ	99.7% (θ = 26.00)	99.6% (θ = 27.01)	100.0% (θ = 25.01)
max. and min. transmn	0.7513 and 0.3766	0.7401 and 0.6451	0.6603 and 0.4647
refinement method	full-matrix least-squares on F^2	full-matrix least-squares on F^2	full-matrix least-squares on F^2
no. of data/restraints/params	2983/0/181	6350/0/334	7182/1/434
goodness-of-fit on F^2	1.041	0.912	0.982
final *R* indices [$I > 2\sigma(I)$]	R_1 = 0.0264, wR_2 = 0.0636	R_1 = 0.0275, wR_2 = 0.0449	R_1 = 0.0392, wR_2 = 0.1043
R indices (all data)	R_1 = 0.0274, wR_2 = 0.0640	R_1 = 0.0331, wR_2 = 0.0459	R_1 = 0.0688, wR_2 = 0.1243
largest diff peak and hole (e·Å^{-3})	1.148 and −1.610	0.871 and −0.440	1.425 and −0.467

catalyze Suzuki coupling of aryl chlorides without the need of stabilizing phosphine ligands.[19] However, the exploration of their reactivity based on the metal−N(R)Py bond was started only recently.[20] In order to gain more insight into the chelating effect, the reactions of **1b** with carbodiimides were also studied. In contrast to **1a**, **1b** reacted with 2 equiv of RN═C═NR under the same conditions to give the unexpected dianionic guanidinate complexes $(Cp_2Yb)_2[\mu\text{-}\eta^2\text{:}\eta^2\text{-PyNC(NR)}_2]$(THF) [R = Cy (**3a**), ^{i}Pr (**3b**)] in yields of 60% and 69% (based on metal), respectively, as bright yellow and orange-red crystals. Presumably, complexes **3a** and **3b** might result from the carbodiimide insertion into the N−H bond of **1b**,[14] followed by the intermolecular guanidine elimination as shown in Scheme 3.

Consistent with this hypothesis, in two cases the elimination products, $PyNC(NHR)_2$, were unambiguously detected and identified by LC/MS, when the reaction residues were extracted with hexane. However, attempts to isolate the intermediates **A** and **B** were unsuccessful. Dianionic guanidinate complexes are rare and are mainly prepared by the cycloaddition of transition metal imido complexes with carbodiimides.[21] Only a few dianionic guanidinate ligands are introduced by deprotonation of monoanionic guanidinates using alkyl[22,23] or amido[23,24] metal reagents, and fewer are found to lead to bridging structures.[22,23] **3a** and **3b** represent the first dianionic guanidinate lanthanide complexes and provide a new insight into the properties of bridged guanidinate metal complexes (vide infra). Although guanidinate metal complexes have been studied extensively, to the best of our knowledge, the analogous guanidine elimination by deprotonation of another guanidinate ligand has not yet been reported. The driving force for the partial guanidine elimination reaction of the putative guanidinate intermediates probably results from the acidity of the N−H proton and the chelating effect of the pyridyl group that seems to favor higher coordination numbers than the corresponding phenyl-substituted guanidinate.[6b] Thus, an additional pyridyl substituent should help to stabilize the bridging coordination of dianionic guanidinate to two Yb^{3+} centers.

Complexes **3a** and **3b** dissolve readily in THF and toluene, but are sparingly soluble in *n*-hexane. The bonding mode of the resulting dianionic guanidinate ligand was proven by the X-ray analysis on complexes **3a** and **3b**. Complexes **3a** and **3b**

(17) (a) Aluarez, C. S.; Bond, A. D.; Harron, E. A.; Layfield, R. A.; McAllister, J. A.; Pask, C. M.; Rawson, J. M.; Wright, D. S. *Organometallics* **2001**, *20*, 4135. (b) Kempe, R. *Eur. J. Inorg. Chem.* **2003**, 791. (c) Standfest-Hauser, C. M.; Mereiter, K.; Schmid, R.; Kirchner, K. *Dalton Trans.* **2003**, 2329. (d) Alvarez, C. S.; Bond, A. D.; Cave, D.; Mosquera, M. E. G.; Harron, E. A.; Layfield, R. A.; McPartlin, M.; Rawson, J. M.; Wood, P. T.; Wright, D. S. *Chem. Commun.* **2002**, 2980. (e) Layfield, R. A.; Bashall, A.; McPartlin, M.; Rawson, J. M.; Wright, D. S. *Dalton Trans.* **2006**, 1660.

(18) (a) Noss, H.; Oberthür, M.; Fischer, C.; Kretschmer, W. P.; Kempe, R. *Eur. J. Inorg. Chem.* **1999**, 2283. (b) Löfgren, A.; Albertsson, A. C.; Dubois, P.; Jerome, R. *J. Macromol. Sci. Rev. Macromol. Chem. Phys.* **1995**, *C35*, 379.

(19) Deeken, S.; Proch, S.; Casini, E.; Braun, H. F.; Mechtler, C.; Marschner, C.; Motz, G.; Kempe, R. *Inorg. Chem.* **2006**, *45*, 1871.

(20) Cole, M. L.; Junk, P. C. *Dalton Trans.* **2003**, 2109.

(21) (a) Ong, T. G.; Yap, G. P. A.; Richeson, D. S. *J. Am. Chem. Soc.* **2003**, *125*, 8100. (b) Zuckerman, R. L.; Bergman, R. G. *Organometallics* **2001**, *20*, 1792. (c) Ong, T. G.; Yap, G. P. A.; Richeson, D. S. *Chem. Commun.* **2003**, 2612. (d) Zuckerman, R. L.; Bergman, R. G. *Organometallics* **2000**, *19*, 4795. (e) Birdwhistell, K. R.; Lanza, J.; Pasos, J. *J. Organomet. Chem.* **1999**, *584*, 200.

(22) Chivers, T.; Parvez, M.; Schatte, G. *J. Organomet. Chem.* **1998**, *550*, 213.

(23) Tin, M. K. T.; Thirupathi, N.; Yap, G. P. A.; Richeson, D. S. *Chem. Commun.* **1999**, 2483.

(24) (a) Tin, M. K. T.; Yap, G. P. A.; Richeson, D. S. *Inorg. Chem.* **1999**, *38*, 998. (b) Bailey, P. J.; Gould, R. O.; Harmer, C. N.; Pace, S.; Steiner, A.; Wright, D. S. *Chem. Commun.* **1997**, 1161.

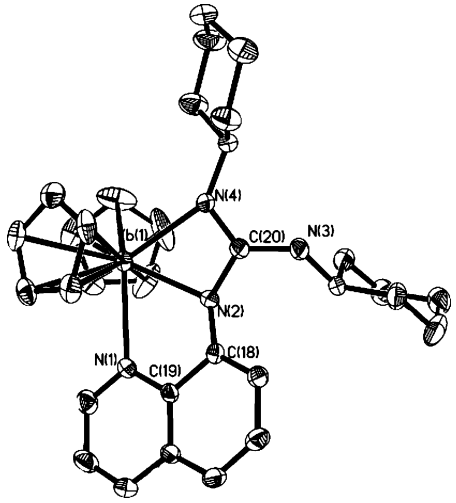

Figure 6. Thermal ellipsoid (30%) plot of complex **2a**. Hydrogen atoms are omitted for clarity. Key bond lengths (Å) and angles (deg): Yb(1)−N(2) 2.265(3), Yb(1)−N(4) 2.447(3), Yb(1)−N(1) 2.508(3), N(2)−C(18) 1.357(4), N(2)−C(20) 1.377(5), N(3)−C(20) 1.377(5), N(4)−C(20) 1.309(5), N(4)−C(20)−N(3) 127.4(4), N(4)−C(20)−N(2) 111.6(4), N(3)−C(20)−N(2) 121.0(4), N(2)−Yb(1)−N(4) 56.1(1).

Scheme 3

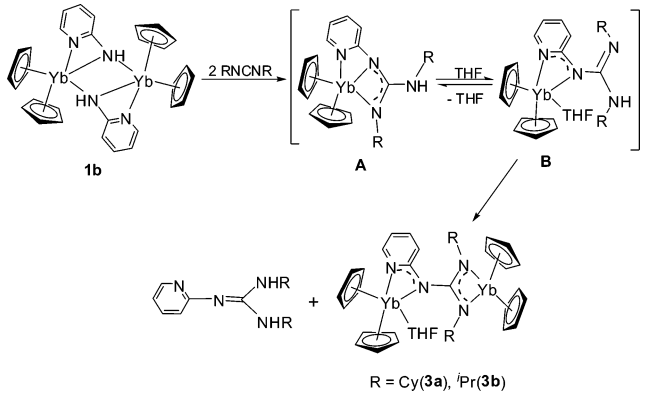

show a characteristic IR absorption band at ca. 1545 cm^{-1} attributable to the −NCN− stretching model of dianionic guanidinate ligands,[22] which is significantly lower than those of monoanionic guanidinate ligands.[25] Also, the N−H stretch that appeared at 3303 cm^{-1} for **1b** was no longer present in **3**. Both **3a** and **3b** are solvated guanidinate-bridged binuclear structures. Although the quality of the structural determination on **3b** was sufficient to unequivocally define the overall connectivity of the atoms, the data were not good enough to allow a detailed discussion of bond distances and angles.

As shown in Figure 7, **3a** is a dinuclear structure possessing one bridging dianionic guanidinate ligand. The two Yb centers possess different coordination environments with Yb(1) being nine-coordinated to two η^5-cyclopentadienyl groups, one THF oxygen, and two nitrogen atoms from pyridyl and the guanidinate bridge, respectively, to give a trigonal bipyramidal geometry, while the Yb(2) atom is coordinated by two η^5-cyclopentadienyl groups and one η^2-guanidinate ligand and its formal coordination number is eight.

The C(15)−N(2) distance (1.37(2) Å) is equivalent to the C(15)−N(1) length, 1.37(2) Å, and shorter than the value of

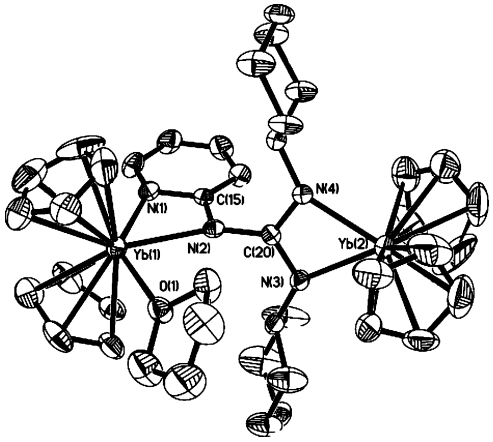

Figure 7. Thermal ellipsoid (30%) plot of complex **3a**. Hydrogen atoms are omitted for clarity. Key bond lengths (Å) and angles (deg): Yb(1)−N(1) 2.36(1), Yb(1)−N(2) 2.38(1), Yb(1)−O(1) 2.40 (1), C(20)−N(3) 1.32(1), C(20)−N(4) 1.35(1), C(20)−N(2) 1.41-(1), C(15)−N(1) 1.37(2), C(15)−N(2) 1.37(2), Yb(2)−N(4) 2.26-(1), Yb(2)−N(3) 2.30(1), N(1)−C(15)−N(2) 110(1), N(3)−C(20)−N(4) 114(1), N(3)−C(20)−N(2) 123(1), N(4)−C(20)−N(2) 124(1), N(2)−Yb(1)−O(1) 79.7(3), N(1)−Yb(1)−N(2) 56.8(3), N(4)−Yb-(2)−N(3) 58.7(3).

Scheme 4. Possible Resonance Structures for Dianionic Guanidinate

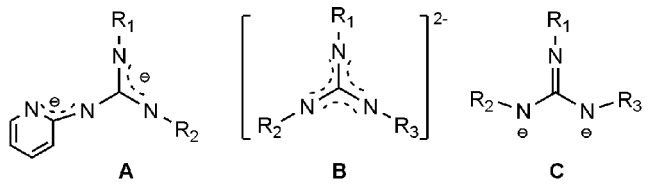

C(20)−N(2), 1.41(1) Å, but slightly longer than the C(20)−N(3) and C(20)−N(4) distances [1.32(1) and 1.35(1) Å, respectively]. These features are consistent with negative charges of the ligand delocalized on the two amidinate units bonded to Yb due to the conjugation effect of the pyridyl substituent (Scheme 4, **A**), whereas in the previously reported dianionic guanidinate complexes the negative charge distribution of the ligands is consistent with the resonance representations **B** and **C** in Scheme 4.[21−24] The average Yb(1)−N distance of 2.37(1) Å is longer than the average Yb(2)−N distance of 2.28(1) Å due to the higher coordination number. All these findings are indicative that a delocalization of ytterbium−nitrogen bonds as in the case of the guanidinate part takes place for the pyridylamido fragment. The $N_{Py}-C-N_{amido}$ angle of 110(1)° instead of the desired 120° or the observed value for amidinato ligands [116(1)°][26] verifies the strained bonding mode.

Reactivity of $[Cp_2Yb(\mu\text{-}\eta^2\text{:}\eta^1\text{-}NHC_6H_4NH_2\text{-}2)]_2$ (1c) toward Carbodiimides. Considering that protonation of guanidinate ligands by other amine substrates is a fundamental step in lanthanide-mediated hydroamination of carbodiimides, the intriguing question of whether intraligand proton transfer is feasible can be raised. To that purpose, we became interested in the reactivity of mixed amino(amido)lanthanide complexes with carbodiimides. The reaction of **1c** with 2 equiv of CyN═C═NCy in THF at room temperature led to the isolation of the single N−H addition product $Cp_2Yb[\eta^1\text{:}\eta^2\text{-}CyNC(NHCy)\text{-}NC_6H_4NH_2\text{-}2]$ (**4a**) in 65% yield, while treatment of **1c** with 4 equiv of CyN═C═NCy gave the double N−H addition product $Cp_2Yb[\eta^1\text{:}\eta^2\text{-}CyNC(NHCy)NC_6H_4\{NC(NHCy)_2\text{-}2\}]$ (**5a**) in 58%

(25) (a) Zhou, Y. L.; Yap, G. P. A.; Richeson, D. S. *Organometallics* **1998**, *17*, 4387. (b) Sirnivas, B.; Chang, C. C.; Chen, C. C.; Chiang, M. Y.; Chen, I. T.; Wang, Y.; Lee, G. H. *J. Chem. Soc., Dalton Trans.* **1997**, 957.

(26) Pi, C. F.; Zhang, Z. X.; Liu, R. T.; Weng, L. H.; Chen, Z. X.; Zhou, X. G. *Organometallics* **2006**, *25*, 5165.

Scheme 5

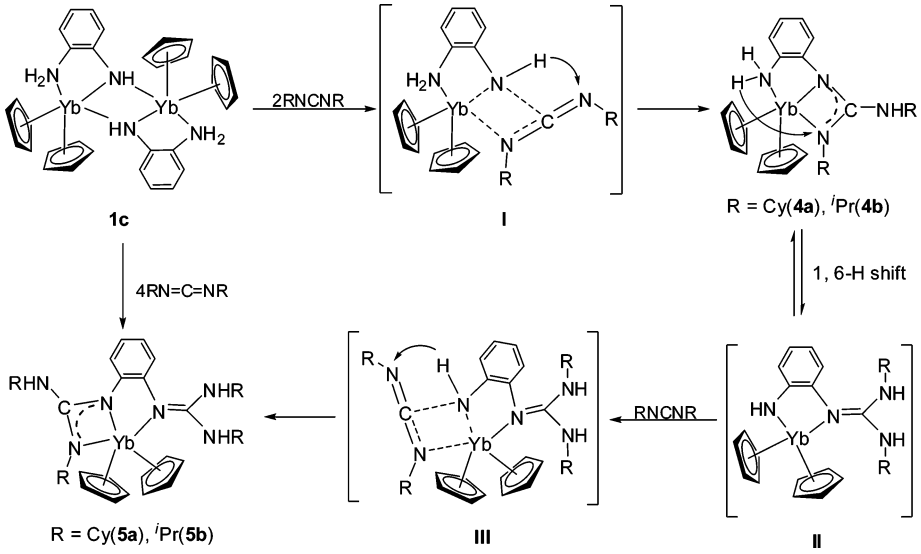

yield. Similarly, **4b** and **5b** can be respectively obtained by controlling the stoichiometric ratio of **1c** and ^{i}PrN═C═N^{i}Pr. It is found that complex **5** could also be obtained by reacting **4** with 1 equiv of RN═C═NR.

A possible reaction pathway for the formation of **4** and **5** is proposed in Scheme 5. In the initial step, coordination of carbodiimide and nucleophilic attack of the amido at the carbodiimide central carbon atom would yield the intermediates **I**.[14,27] Then, the 1,3-hydrogen migration from the amido to the more basic uncoordinated nitrogen affords the formal single N−H bond addition products **4**. Furthermore, an intraligand proton transfer from the chelating NH_2 group to the metal-bound guanidinate group[8,28] and subsequent formal insertion of a second carbodiimide molecule into the N−H bond of the newly formed amido group yields the double N−H addition products **5**. To the best of our knowledge, the formation of compounds **5** is a rare example of multiple N−H activation of organolanthanides, which provides an effective method for stepwise guanylation of polyamido and/or amino lanthanide complexes.

An ORTEP diagram of **4b** is shown in Figure 8. Complex **4b** is a solvent-free mononuclear structure with the ytterbium atom bonded to two η^5-cyclopentadienyl rings, two N atoms from the guanidinate anion, and one amino N atom. In contrast to the observations in simple guanidinate lanthanide complexes, where the π-electrons of the C═N double bond of the guanidinate group are delocalized over the N−C−N unit, in **4b** the N(1)−C(14) and N(2)−C(14) distances of 1.312(7) and 1.369(6) Å in the YbN_2C ring suggest a tendency toward CN double and single bonds, respectively (cf. mean values of 1.36 Å for C(sp^2)−N and 1.29 Å for C(sp^2)═N) and limited delocalization of negative charge.[15] Consistent with this observation, the Yb(1)−N(2) and Yb(1)−N(1) distances, 2.286(5) and 2.416(5) Å, feature the expected Yb−N "σ-bond" distance and donor-bond distance, respectively. The exocyclic C(14)−N(3) bond length of 1.360(6) Å is consistent with a C(sp^2)−N single bond and the presence of a hydrogen atom on the exocyclic nitrogen. The sum of the bond angles at the central carbon atom C(14) is close to 360°. The Yb(1)−N(4) distance of 2.501(5) Å is similar to those observed for $Cp_2ZYb-NR_3$ donor bonds (Z = monoanionic ligand).[10a,b] No unusual distance and angle in the Cp_2Yb unit is found in **4b**.

The results summarized in Figure 9 confirm the proposed structure of complex **5a** and reveal that CyN═C═NCy is inserted into the N−H bond of all the available amido groups via an intraligand proton transfer reaction. The Yb coordination environment is composed of a trisubstituted bidentate momoanionic guanidinate group, one monodentate neutral guanidine, and two η^5-Cp groups. The guanidinate anion is bonded to Yb through the N(1) and N(2) to yield a planar four-membered ring of sp^2-hybridized N and C. The Yb−N(1) distance, 2.227(3) Å, is significantly shorter than the Yb−N(2) distance, 2.484(3) Å, indicating asymmetry in the coordination of this ligand to Yb^{3+}. This asymmetry is further reflected in the ligand, where the N(1)−C(11) distance of 1.353(5) Å is slightly longer than the N(2)−C(11) distance, 1.304(4) Å. These two observations suggest a substantial contribution to the static structure of **5a** from the localized bonding. A similar asymmetric bonding feature has been observed for $TaCl(NMe_2)_3\{[(CH_3)_2CHN]_2CN(H)CH(CH_3)_2\}$.[29] The Yb−N(4) distance, 2.476(3) Å, compares favorably with those reported for the Yb ←:N donor bond distances.[10a,b]

Attempts were also made to obtain structural information in the solid state of **5b**, but the poor quality of the obtained crystals prevented any X-ray determination.

Reaction of $[Cp_2Yb\{\mu\text{-}\eta^2\text{:}\eta^1\text{-}NHC_5H_3N(NH_2\text{-}3)\}]_2$ (1d) with CyN═C═NCy. Tandem N−H activation of amines is the key step in the catalytic hydroamination. Consequently, a good understanding of the factors that promote or deter multiple N−H activation would permit one to control this reaction and enable design of new catalysts for hydroamination of unsaturated substrates. Recently, metal-catalyzed guanylation of carbodiimides has attracted increasing interest.[28] However, little is known about the structures and reactivities of initially formed reactive intermediates in these courses. [28,30] In addition, the type of ligand-based N−H addition process has not been authenticated previously for other metal-catalyzed guanylation of carbodiimides. To obtain additional insight into the mechanism

(27) Vicente, J.; Abad, J. A.; López-Sáez, M. J. *Organometallics* **2006**, *25*, 1851.

(28) (a) Montilla, F.; del Río, D.; Pastor, A.; Galindo, A. *Organometallics* **2006**, *25*, 4996. (b) Shen, H.; Chan, H. S.; Xie, Z. *Organometallics* **2006**, *25*, 5515. (c) Ong, T. G.; O'Brien, J. S.; Korobkov, I.; Richeson, D. S. *Organometallics* **2006**, *25*, 4728.

(29) Tin, M. K. T.; Thirupathi, N.; Yap, G. P. A.; Richeson, D. S. *J. Chem. Soc., Dalton Trans*. **1999**, 2947.

(30) Zhang, W. X.; Nishiura, M.; Hou, Z. M. *Chem. Commun.* **2006**, *36*, 3812.

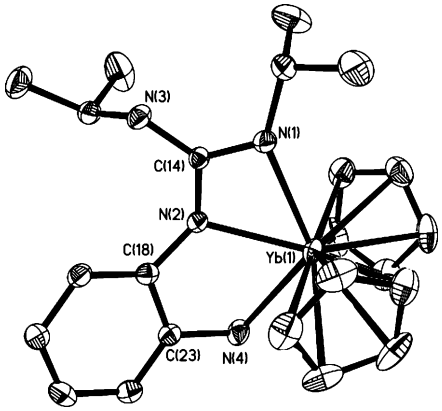

Figure 8. Thermal ellipsoid (30%) plot of complex **4b**. Hydrogen atoms are omitted for clarity. Key bond lengths (Å) and angles (deg): Yb(1)−N(2) 2.286(5), Yb(1)−N(1) 2.416(5), Yb(1)−N(4) 2.501(5), N(1)−C(14) 1.312(7), N(2)−C(14) 1.369(6), N(2)−C(18) 1.385(7), N(2)−C(18) 1.385(7), N(3)−C(14) 1.360(6), N(2)−Yb(1)−N(1) 56.2(2), N(2)−Yb(1)−N(4) 65.1(2), N(1)−C(14)−N(3) 126.2(5), N(1)−C(14)−N(2) 111.2(5), N(3)−C(14)−N(2) 122.6(5).

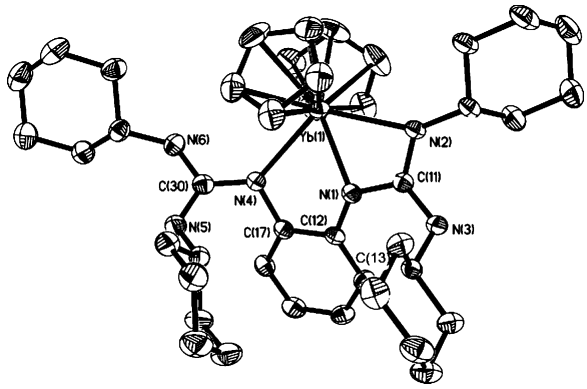

Figure 9. Thermal ellipsoid (30%) plot of complex **5a**. Hydrogen atoms are omitted for clarity. Key bond lengths (Å) and angles (deg): Yb(1)−N(1) 2.227(3), Yb(1)−N(2) 2.484(3), Yb(1)−N(4) 2.476(3), N(1)−C(11) 1.353(5), N(2)−C(11) 1.304(4), N(3)−C(11) 1.382(5), N(4)−C(30) 1.327(5), N(5)−C(30) 1.363(5), N(6)−C(30) 1.362(5), N(1)−C(12) 1.382(4), N(4)−C(17) 1.425(5), N(1)−Yb(1)−N(2) 55.4(1), N(2)−C(11)−N(1) 112.1(4), N(2)−C(11)−N(3) 126.7(4), N(1)−C(11)−N(3) 121.1(3), N(4)−C(30)−N(6) 117.6(4), N(4)−C(30)−N(5) 124.4(4), N(6)−C(30)−N(5) 118.0(4).

and scope of the reaction, we decided to extend our study to the double guanylation of lanthanide complexes containing hybrid amino/amido ligands. Interestingly, by replacement of *o*-aminophenylamido with 3-aminopyridylamido, which has combined characteristics of *o*-aminophenylamido and 2-pyridylamido, the double-addition product **6** could be obtained as red crystals from the 1:4 reaction between **1d** and CyN═C═NCy in a good yield with complete chemoselectivity. A pathway similar to that proposed for the formation of **5** is very likely to account for the formation of **6**. Namely, the first step in this multiple N−H bond activation system is a CyN═C═NCy insertion into the N−H bond of the amido of **1d**, giving **i** as a transient intermediate. **i** could adopt an **ii** structure with the aid of additional intramolecular hydrogen bonding. As soon as **iii** is formed by intramolecular proton transfer, it could then insert into a second CyN═C═NCy to form **iv**. Last, the converse 1,8-H shift gives the more stable compound **6**. Although no pure monoinsertion intermediate has been isolated, it was observed by LC-MS analysis of hydrolysis products of the reaction mixture.

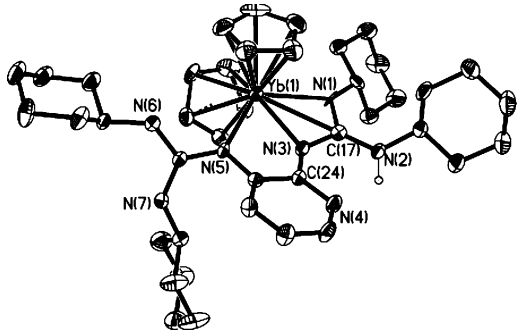

Figure 10. Thermal ellipsoid (30%) plot of complex **6**. Hydrogen atoms are omitted for clarity [except for N(2)]. Key bond lengths (Å) and angles (deg): Yb(1)−N(3) 2.247(9), Yb(1)−N(5) 2.482(9), Yb(1)−N(1) 2.522(8), N(1)−C(17) 1.399(13), N(2)−C(17) 1.360(14), N(3)−C(17) 1.350(14), N(5)−C(35) 1.337(13), N(6)−C(35) 1.341(14), N(7)−C(35) 1.341(14), N(3)−C(24) 1.349(13), N(2)···N(4) 2.749, N(4) ···H(2) 2.261, N(2)−H(2)···N(4) 115.86, N(3)−C(17)−N(2) 120.7(9), N(3)−C(17)−N(1) 113.3(9), N(2)−C(17)−N(1) 125.9(10), N(5)−C(35)−N(6) 116.5(9), N(5)−C(35)−N(7) 124.9(10), N(6)−C(35)−N(7) 118.6(10), N(3)−Yb(1)−N(5) 66.3(3), N(3)−Yb(1)−N(1) 57.2(3).

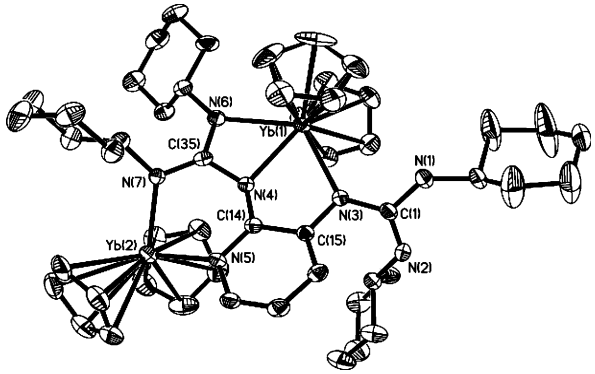

Figure 11. Thermal ellipsoid (30%) plot of complex **7**. Hydrogen atoms are omitted for clarity. Key bond lengths (Å) and angles (deg): Yb(1)−N(4) 2.265(5), Yb(1)−N(6) 2.391(6), Yb(1)−N(3) 2.432(5), Yb(2)−N(7) 2.267(5), Yb(2)−N(5) 2.329(6), N(3)−C(15) 1.410(8), N(7)−C(35) 1.360(8), N(4)−C(35) 1.380(8), N(6)−C(35) 1.314(8), N(4)−C(14) 1.355(8), N(5)−C(14) 1.351(8), N(3)−C(1) 1.341(8), N(3)−C(15) 1.410(8), N(6)−C(35)−N(7) 131.7(6), N(6)−C(35)−N(4) 107.4(6), N(7)−C(35)−N(4) 120.9(6).

It is of interest to note that the nature of rings regulates the hydrogen migration. A major difference with respect to complexes **5** is that complex **6** features a converse hydrogen migration. Presumably, in the formation of **6** the driving force for the additional converse 1,8-H shift of the putative guanidinate intermediate probably results from the stronger acidity of the guanidine group at the 2-position as compared with that at the 3-position. These results again demonstrate that substantial proton transfer from amino to guanidinate is required in the above double-guanylation processes.

Complex **6** dissolves readily in THF and toluene and is only sparingly soluble in *n*-hexane. The X-ray crystallographic analysis reveals that the coordination geometry around the metal center is approximately trigonal bipyramidal, with the two Cp centers and one N atom in equatorial positions (Figure 10). Interestingly, complex **6**, like pyridyl thioureas,[31] is found in a conformation of the Cy substituent on the N(2) atom lying opposite of the N(4) atom, resulting from intramolecular hydrogen bonding of N(2)−H to the pyridine nitrogen N(4), while in **5a** the Cy substituent on the N(3) atom lies at the adjacent position of the C(13) atom. N(2)−H···N(4) hydrogen

Scheme 6

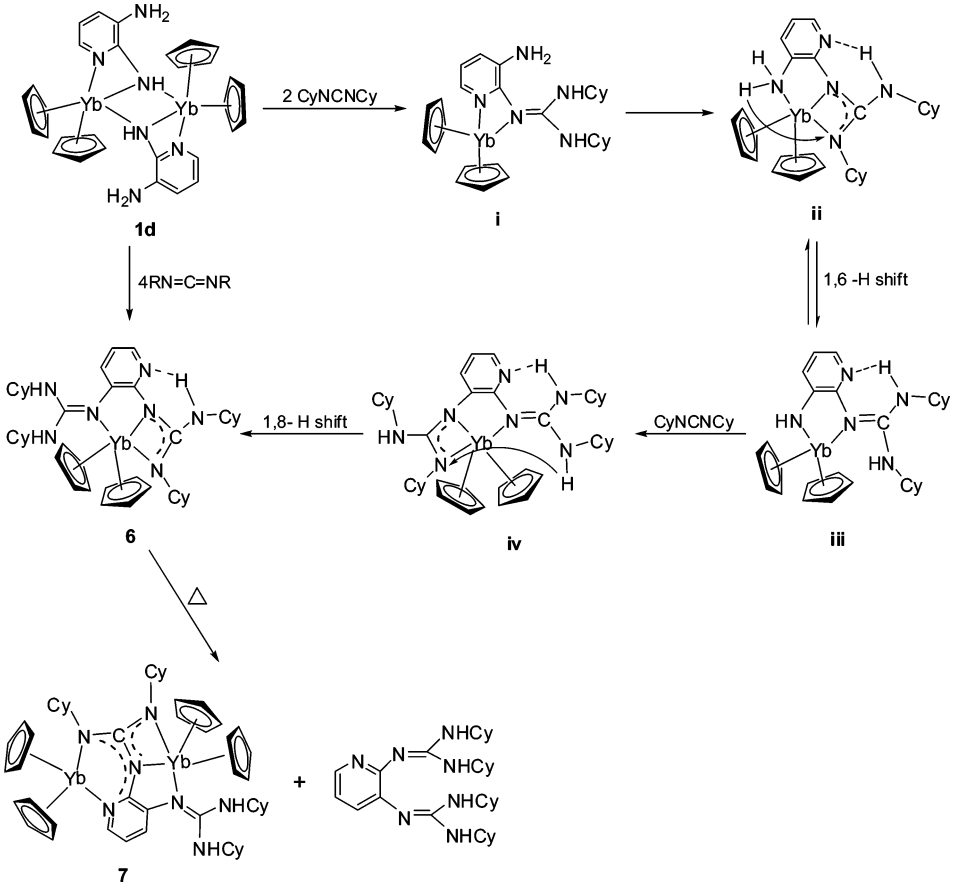

Scheme 7

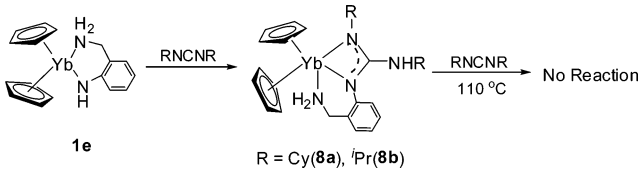

bonding occurs at a distance of 2.749 Å, and it appears to be formed by the symmetry-related amino H atom and nitrogen atom of the parental pyridyl ring. The N(2)−H···N(4) intramolecular interaction has a longer N···N distance than the corresponding distance found in pyridyl thioureas [2.610(6)−2.688(6) Å],[32] indicating that the Yb atom coordinations to N(1), N(3), and N(5) cause a substantial elongation of the intramolecular hydrogen bond. As a result, the Yb(1)−N(1) distance of 2.522(8) Å is slightly longer than the corresponding value of 2.484(3) Å in **5a**.

Interestingly, in contrast to **5a**, complex **6** is unstable to heat and is readily transformed to the unusual neutral guanidine-substituted guanidinate dianion lanthanide complex **7** under refluxing in THF with intermolecular elimination of neutral diguanidine, as indicated in Scheme 6. Both the formation and the abstraction of guanidinate ligands are important steps in metal-mediated guanylation of amines. Thus, the sequential formations of **1d**, **6**, **7**, and diguanidine provide an insight into the complete organolanthanide-catalyzed diguanylation reaction course of diamines. Furthermore, these results demonstrate that the chelating effect of pyridyl rings can impart the guanidinate complexes a unique reactivity and initiates the unexpected reaction sequence.

Positive structural verification of **7** was also provided by a single-crystal X-ray analysis (Figure 11). In contrast to the observation in **3a**, where the pyridyl-substituted guanidinate dianion ligand forms two planar four-membered rings with two ytterbium atoms with the negative charges delocalized on the two amidinate units bonded to Yb independently as shown in Scheme 3, in the present complex the pyridyl-substituted guanidinate dianion ligand forms respectively one four-membered ring and one six-membered ring with two Yb metals with the negative charge distribution over the C_2N_4 unit. This difference may result from the chelating effect of the guanidine substituent on the 3-position of the pyridyl ring.

Reactivity of $Cp_2Yb[\eta^1:\eta^1\text{-}NHC_6H_4(CH_2NH_2\text{-}2)]$ (1e) toward Carbodiimides. In order to confirm that the proton transfer is really preferred over the second carbodiimide insertion into the N−H bond in the formation of **5** and **6**, we also synthesized the relative aminomethyl-substituted arylamido complex **1e** and examined its reaction with carbodiimides. By treatment of **1e** with a stoichiometric amount of RN═C═NR in THF, the monoinsertion products $Cp_2Yb[\eta^2:\eta^1\text{-}CyNC(NHCy)\text{-}NC_6H_4(CH_2NH_2\text{-}2)]$ (R = Cy (**8a**), ^{i}Pr (**8b**)) were easily obtained in high yield under mild reaction conditions (Scheme 7).

(31) (a) Corbin, P. S.; Zimmerman, S. C. *J. Am. Chem. Soc.* **2000**, *122*, 3779. (b) West, D. X.; Swearingen, J. K.; Hermetet, A. K.; Ackerman, L. J.; Presto, C. *J. Mol. Struct.* **2000**, *522*, 27. (c) Corbin, P. S.; Zimmerman, S. C.; Thiessen, P. A.; Hawryluk, N. A.; Murray, T. J. *J. Am. Chem. Soc.* **2001**, *123*, 10475. (d) Kaminsky, W.; Kelman, D. R.; Giesen, J. M.; Goldberg, K. I.; Claborn, K. A.; Szczepura, L. F.; West, D. X. *J. Mol. Struct.* **2002**, *616*, 79. (e) Hermetet, A. K.; Ackerman, L. J.; Swearingen, J. K.; Presto, C. A.; Kelman, D. R.; Giesen, J. M.; Goldberg, K. I.; Kaminsky, W.; West, D. X. *J. Chem. Crystallogr.* **2002**, 3217. (f) Chien, C.; Leung, M.; Su, J.; Li, G.; Liu, Y.; Wang, Y. *J. Org. Chem.* **2004**, *69*, 1866.

(32) Kelman, D. R.; Claborn, K. A.; Kaminsky, W.; Goldberg, K. I.; West, D. X. *J. Mol. Struct.* **2002**, *642*, 119.

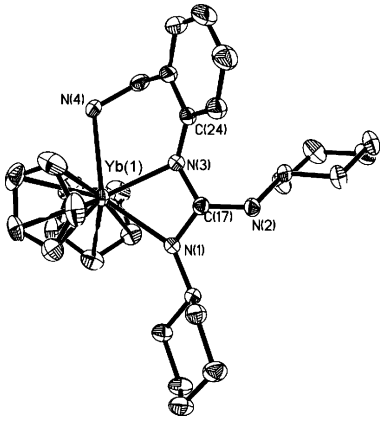

Figure 12. Thermal ellipsoid (30%) plot of complex **8a**. Hydrogen atoms are omitted for clarity. Key bond lengths (Å) and angles (deg): Yb(1)−N(3) 2.291(4), Yb(1)−N(1) 2.405(4), Yb(1)−N(4) 2.492(4), N(3)−C(24) 1.402(6), N(1)−C(17) 1.313(5), N(2)−C(17) 1.369(5), N(3)−C(17) 1.358(6), N(1)−C(17)−N(3) 113.4(4), N(1)−C(17)−N(2) 125.0(4), N(3)−C(17)−N(2) 121.6(4), N(3)−Yb(1)−N(1) 56.7(1).

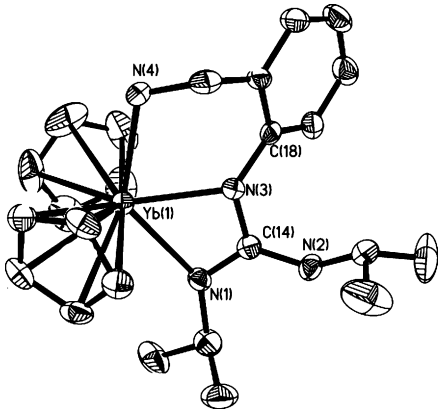

Figure 13. Thermal ellipsoid (30%) plot of complex **8b**. Hydrogen atoms are omitted for clarity. Key bond lengths (Å) and angles (deg): Yb(1)−N(3) 2.293(3), Yb(1)−N(1) 2.417(3), Yb(1)−N(4) 2.474(4), N(3)−C(18) 1.405(5), N(3)−C(14) 1.364(5), N(1)−C(14) 1.308(5), N(2)−C(14) 1.368(5), N(1)−C(14)−N(3) 112.5(4), N(1)−C(14)−N(2) 124.5(4), N(3)−C(14)−N(2) 123.1(4), N(3)−Yb(1)−N(1) 56.2(1).

However, attempts to isolate the di-insertion products similar to **5** were unsuccessful, even when a large excess of carbodiimide was added under forcing conditions. It is interesting to note that, in marked contrast to **4**, the amino group of **8a** and **8b** is inert and undergoes neither the direct addition to excess RN═C═NR (R = Cy, ^{i}Pr) that occurs directly at the free NH_2 group[33] nor the proton transfer to the newly formed guanidinate ligand under the conditions involved. Obviously, this may be attributed to both its lower nucleophilicity caused by the chelating coordination and inherent weak acidity.

A tandem addition/proton transfer/re-addition reaction is observed in the treatment of **1c** and **1d** with excess carbodiimides, whereas for **1e** only the monoaddition reaction is observed in the presence of excess carbodiimides even with prolonged heating at 110 °C. Considering that aliphatic amines more easily undergo direct addition with carbodiimides to yield *N*,*N*,*N*-trialkylguanidines than aromatic amines in organic synthesis and that aromatic amines have a stronger acidity compared with aliphatic amines,[28a,33] these results are consistent with the relative acidity of aromatic amine > aliphatic amine and thus also provide evidence to support the mechanistic consideration that the proton transfer from the coordinated amino group to the newly formed guanidinate group is the driving force for the further hydroamination reaction of the monoaddition intermediate with carbodiimide in the formation of **5** and **6**. Since aliphatic NH_2 is not acidic enough to protonolyze the aryl-substituted guanidinate ligand, re-forming an amido group, the further guanylation for **8** is prevented.

X-ray-quality crystals of **8a** and **8b** were obtained by slowly cooling their saturated THF solution, and the resultant structures confirm the connectivity in the complexes (Figures 12 and 13). Indeed, only the amido in **8** has undergone the addition of a N−H bond across the carbon−nitrogen double bond of the carbodiimide to form a new guanidinate ligand, which is coordinated to the lanthanide ion in an η^2-fashion. Geometric parameters involving the Yb atom in **8a** are similar to those found in **8b**, although there are some distinctions. The Yb−N(NH_2) distances in **8** [**8a** 2.474(4) Å, **8b** 2.492(4) Å] are noticeably longer than the corresponding value in **1e** [2.395(5) Å] and are similar to the values found in **4b**.

Conclusions

In summary, a series of new ytterbium complexes containing different functionalized primary amido ligands such as 8-quinolylamido, 2-pyridylamido, 2-aminoarylamido, 3-aminopyridylamido, and 2-aminomethylarylamido are prepared by salt metathesis of $[Cp_2YbCl]_2$ and the corresponding amido lithium. We have found that these complexes exhibit intriguing reactivity toward carbodiimides owing to the accessibility of multiple N−H activation for metal-bound neutral NH_2 and anionic nitrogen-containing fragments. The amino group in the *ortho* position not only introduces chelating ability but induces some unusual tandem reactions, while the presence of the pyridyl group tends to increase the coordination and acidity available in the guanidinate ligand, thereby providing a driving force for the transformation of monoanionic guanidinate to dianionic guanidinate. These differences demonstrate that the nature of the functional group at the amido ligands often exerts a significant influence on the outcome of the reaction. Furthermore, the present work provides a detailed insight into general mechanistic aspects of the metal-mediated mono- and diguanylation of primary amines and elucidates factors that affect the chemo- and regioselectivities, since protonation of guanidinate and N−H addition to carbodiimide are the two most fundamental steps in the catalytic cycles.

Significant efforts have been made to develop reliable synthetic routes to guanidinate complexes. Their role as intermediates in important transformations such as guanylation and C−N coupling reactions has called for mechanistic investigations into the chemical reactivity of metal amido species. Although the chemistry of delocalized guanidinate ligands is being developed, it is limited primarily to simple guanidinate ligands.[16,34] Very few reports are available on bridged bis(guanidinate) complexes.[33,35] We are aware of no examples of characterized bridged bis(guanidinate) lanthanide or yttrium

(33) (a) Fulton, J. R.; Holland, A. W.; Fox, D. J.; Bergman, R. G. *Acc. Chem. Res*. **2002**, *35*, 44. (b) Uevia, E.; Pérez, J.; Riera, V. *Organometallics* **2003**, *22*, 257. (c) Uevia, E.; Pérez, J.; Riera, V.; Miguel, D. *Chem. Commun.* **2002**, 1814.

(34) (a) Bailey, P. J.; Pace, S. *Coord. Chem. Rev.* **2001**, *214*, 91. (b) Coles, M. P.; Hitchcock, P. B. *Dalton Trans*. **2001**, 1169. (c) Lu, Z.; Yap, G. P. A.; Richeson, D. S. *Organometallics* **2001**, *20*, 706.

(35) (a) Mansfield, N. E.; Coles, M. P.; Avent, A. G.; Hitchcock, P. B. *Organometallics* **2006**, *25*, 2470. (b) Foley, S. R.; Yap, G. P. A.; Richeson, D. S. *Inorg. Chem.* **2002**, *41*, 4149.

complexes, which is somewhat surprising considering the extensive use of the bridged bis(cyclopentadienyl),[36] bis(amido),[37] and bis(aryloxide)[38] analogues with these metals. The present double-guanylation reaction not only demonstrates the potential of the hybrid amino/amido ligand in further functionalization but also portends that bridged bis(guanidinate) mono- and dianion lanthanide complexes might be synthesized.

In brief, this work highlights the distinctive reactivity of the hybrid amino/amido ligands and exemplifies their potential in stepwise functionalizations, demonstrating that conversion of the monoanionic guanidinate into the dianionic guanidinate ligand can rationally be induced by the proton transfer between anionic guanidinate ligands, as indicated in the formation of complexes **3** and **7**.

Experimental Section

General Remarks. All operations involving air- and moisture-sensitive compounds were carried out under an inert atmosphere of purified nitrogen gas using standard Schlenk techniques. The solvents THF, toluene, and *n*-hexane were refluxed and distilled over sodium benzophenone ketyl under nitrogen gas prior to use. Elemental analyses for C, H, and N were carried out by using a Rapid CHN-O analyzer. Infrared spectra were obtained on a Nicolet FTIR 360 spectrometer with samples prepared as Nujol mulls. $[Cp_2YbCl]_2$ was prepared according to the reported method.[39] The lithiated anilines, LiNHAr, were prepared according to the modified procedures described in the literature[40] by adding 1 molar equiv of ^{n}BuLi to a *n*-hexane solution of the appropriate aniline. This mixture was dried in vacuo after 2 h of stirring, rinsed with *n*-hexane, and used without further purification. All the arylamines and carbodiimidines were purchased from commercial sources and were used without further purification.

Preparation of $[Cp_2Yb(\mu\text{-}\eta^2\text{:}\eta^1\text{-NHQu})]_2$ (1a). To a solution of $[Cp_2YbCl]_2$ (0.630 g, 0.93 mmol) in 60 mL of toluene was added LiNHQu (0.279 g, 1.86 mmol) at −30 °C. After stirring for 30 min at low temperature, the reaction solution was slowly warmed to room temperature and stirred for another 12 h. Then the precipitate was removed by centrifugation and the clear solution was concentrated by reduced pressure until a precipitate formed. The precipitate was redissolved and the solution stored at −15 °C (a few days), resulting in the formation of orange-red crystals of **1a**. Yield: 0.490 g (59%). Anal. Calcd for $C_{38}H_{34}N_4Yb_2$: C, 51.12; H, 3.84; N, 6.28. Found: C, 51.10; H, 3.81; N, 6.26. IR (Nujol, cm^{-1}): 3558 (w), 3385 (w), 3064 (w), 1596 (w), 1567 (m), 1505 (s), 1315 (vs), 1263(m), 1094 (m), 1016 (m), 892 (w), 785 (s), 664 (m).

Preparation of $[Cp_2Yb(\mu\text{-}\eta^2\text{:}\eta^1\text{-NHPy})]_2$ (1b). Following the procedure described for **1a**, using $[Cp_2YbCl]_2$ (0.569 g, 0.84 mmol) and LiNHPy (0.168 g, 1.68 mmol) afforded **1b** as red crystals. Yield: 0.466 g (70%). Anal. Calcd for $C_{30}H_{30}N_4Yb_2$: C, 45.33; H, 3.81; N, 7.05. Found: C, 45.20; H, 3.79; N, 7.01. IR (Nujol, cm^{-1}): 3556 (w), 3303 (m), 3075 (w), 3020 (w), 1604 (vs), 1556 (s), 1435 (vs), 1311(s), 1277 (w), 1297 (w), 1146 (m), 1012 (s), 864 (m), 770 (s), 736 (m).

Preparation of $[Cp_2Yb(\mu\text{-}\eta^2\text{:}\eta^1\text{-NHC}_6H_4NH_2\text{-}2)]_2$ (1c). Following the procedure described for **1a**, using $[Cp_2YbCl]_2$ (0.677 g, 1.00 mmol) and $LiNHC_6H_4NH_2$-2 (0.228 g, 2.00 mmol) gave **1c** as orange crystals. Yield: 0.540 g (62%). Anal. Calcd for $C_{32}H_{34}N_4Yb_2$: C, 46.83; H, 4.18; N, 6.83. Found: C, 46.63; H, 4.15; N, 6.79. IR (Nujol, cm^{-1}): 3326 (w), 3293 (s), 3250 (vs), 3066 (m), 3025 (m), 1603 (s), 1561 (s), 1492 (s), 1326 (m), 1257 (s), 1179 (s), 1099 (s), 1014 (vs), 894 (w), 863 (m), 746 (s), 655 (s), 587 (s).

Preparation of $[Cp_2Yb\{\mu\text{-}\eta^2\text{:}\eta^1\text{-NHC}_5H_3N(NH_2\text{-}3)\}]_2$ (1d). Following the procedure described for **1a**, using $[Cp_2YbCl]_2$ (0.562 g, 0.83 mmol) and $LiNHC_5H_3N(NH_2$-3) (0.191 g, 1.66 mmol) gave **1d** as orange crystals. Yield: 0.397 g (58%). Anal. Calcd for $C_{30}H_{34}N_6Yb_2$: C, 43.69; H, 4.16; N, 10.19. Found: C, 43.66; H, 4.11; N, 10.12. IR (Nujol, cm^{-1}): 3433 (w), 3398 (s), 3335 (s), 3076 (m), 1560 (s), 1282 (s), 1078 (m), 1013(s), 896 (w), 793 (vs), 762 (s), 726 (m), 587 (m).

Preparation of $Cp_2Yb[\eta^1\text{:}\eta^1\text{-NHC}_6H_4(CH_2NH_2\text{-}2)]$ (1e). Following the procedure described for **1a**, reaction of $[Cp_2YbCl]_2$ (0.677 g, 1.00 mmol) with 2 equiv of $LiNHC_6H_4(CH_2NH_2$-2) (0.256 g, 2.00 mmol) gave **1e** as red crystals. Yield: 0.289 g (68%). Anal. Calcd for $C_{17}H_{19}N_2Yb$: C, 48.11; H, 4.51; N, 6.60. Found: C, 47.93; H, 4.48; N, 6.55. IR (Nujol, cm^{-1}): 3401 (m), 3355 (m), 3301 (m), 3257 (s), 3068 (m), 1621 (m), 1587 (s), 1490 (s), 1324 (m), 1298 (s), 1219 (w), 1155 (m), 1117 (m), 1075 (m), 1009 (m), 970 (m), 922 (s), 891 (m), 752 (vs), 665(s).

Preparation of $Cp_2Yb[\eta^2\text{:}\eta^1\text{-CyNC(NHCy)NQu}]$ (2a). To a solution of **1a** (0.540 g, 0.55 mmol) in 40 mL of THF was added *N*,*N*′-dicyclohexylcarbodiimide (0.227 g, 1.1 mmol) at ambient temperature. After stirring for 12 h, the solvent was evaporated under vacuum, leaving a red-orange residue, which was washed with hexane (5 mL × 3). Then, the resulting solid was extracted with toluene (20 mL × 2). The extractants were combined and concentrated to about 10 mL, from which **2a** was obtained as a red-orange powder at −15 °C. Diffusion of hexane into a solution of **2a** in THF afforded 0.546 g of orange-red crystals. Yield: 0.546 g (76%). Anal. Calcd for $C_{32}H_{39}N_4Yb$: C, 58.78; H, 6.02; N, 8.57. Found: C, 58.65; H, 5.98; N, 8.52. IR (Nujol, cm^{-1}): 3347 (m), 3085 (w), 3072 (w), 3046 (w), 1596 (m), 1559(s), 1497 (s), 1409 (s), 1363(m), 1348 (m), 1331 (m), 1310 (m), 1299 (m), 1283, 1262 (m), 1241 (m), 1189 (w), 1146 (m), 1136, 1071 (m), 1011 (m), 978 (w), 891 (w), 866 (w), 823 (m), 795 (m), 783 (m), 760 (s), 741 (w), 648 (w).

Preparation of $Cp_2Yb[\eta^2\text{:}\eta^1\text{-}^i\text{PrNC(NH}^i\text{Pr)NQu}]$ (2b). Following the procedure described for **2a**, reaction of **1a** (0.484 g, 0.54 mmol) and *N*,*N*′-diisopropylcarbodiimide (0.136 g, 1.08 mmol) followed by crystallization from THF/hexane afforded **2b** as orange-red crystals. Yield: 0.433 g (70%). Anal. Calcd for $C_{26}H_{31}N_4Yb$: C, 54.54; H, 5.46; N, 9.78. Found: C, 54.47; H, 5.43; N, 9.72. IR (Nujol, cm^{-1}): 3340 (m), 3079 (w), 3070 (w), 3050 (w), 1610 (m), 1561(s), 1490 (s), 1410 (s), 1358(m), 1350 (m), 1325 (m), 1310 (m), 1295 (m), 1280, 1243 (m), 1192 (w), 1145 (m), 1010 (m), 978 (w), 890 (w), 876 (w), 820(m), 795 (m), 760 (s), 755 (w).

Preparation of $(Cp_2Yb)_2[\mu\text{-}\eta^2\text{:}\eta^2\text{-PyNC(NCy)}_2](THF)$ (3a). Following the procedure described for **2a**, **1b** (0.666 g, 0.84 mmol) reacted with *N*,*N*′-dicyclohexylcarbodiimide (0.347 g, 1.68 mmol) to afford 0.492 g of bright yellow crystals of **3a**. Yield: 60% (based on Yb). Anal. Calcd for $C_{42}H_{54}N_4OYb_2$: C, 51.63; H, 5.57; N, 5.73. Found: C, 51.47; H, 5.53; N, 5.68. IR (Nujol, cm^{-1}): 3091 (m), 1067 (s), 1545 (w), 1434 (vs), 1394 (vs), 1359 (s), 1294 (m), 1258 (w), 1210 (m), 1154 (m), 1078 (w), 1056 (m), 954 (w), 865 (w), 788 (s), 765 (s).

Preparation of $(Cp_2Yb)_2[\mu\text{-}\eta^2\text{:}\eta^2\text{-PyNC(N}^i\text{Pr)}_2](THF)$ (3b). Following the procedure described for **2a**, treatment of **1b** (0.618 g, 0.78 mmol) with *N*,*N*′-diisopropylcarbodiimide (0.197 g, 1.56

(36) (a) Qian, C. T.; Nie, W. L.; Sun, J. *J. Organomet. Chem.* **2001**, *626*, 171. (b) Qian, C. T.; Nie, W. L.; Chen, Y. F.; Sun, J. *J. Organomet. Chem.* **2002**, *645*, 82. (c) Nie, W. L.; Qian, C. T.; Chen, Y. F.; Sun, J. *J. Organomet. Chem.* **2002**, *647*, 114. (d) Qian, C. T.; Zou, G.; Gao, L. *J. Organomet. Chem.* **1996**, *525*, 23.

(37) Zhou, L. Y.; Yao, Y. M.; Li, C.; Zhang, Y.; Shen, Q. *Organometallics* **2006**, *25*, 2880.

(38) (a) Wang, Z. G.; Sun, H. M.; Yao, H. S.; Yao, Y. M.; Shen, Q.; Zhang, Y. *J. Organomet. Chem.* **2006**, *691*, 3383. (b) Schaverien, C. J.; Meijboom, N.; Orpen, A. G. *J. Chem. Soc., Chem. Commun.* **1992**, 124. (c) Yao, Y. M.; Xu, X. P.; Liu, B.; Zhang, Y.; Shen, Q.; Wong, W. T. *Inorg. Chem.* **2005**, *44*, 5133. (d) Deng, M. Y.; Yao, Y. M.; Shen, Q.; Zhang, Y.; Sun, J. *Dalton Trans.* **2004**, 944.

(39) Maginn, R. E.; Manastryskyj, S.; Dubeck, M. *J. Am. Chem. Soc.* **1963**, *85*, 672.

(40) Eckert, N. A.; Smith, J. M.; Lachicotte, R. J.; Holland, P. L. *Inorg. Chem.* **2004**, *43*, 3306.

Table 3. Crystal and Data Collection Parameters of Complexes 4b, 5a, and 6

	4b	**5a**·2THF	**6**·THF
formula	$C_{23}H_{31}N_4Yb$	$C_{50}H_{77}N_6O_2Yb$	$C_{45}H_{68}N_7OYb$
molecular weight	536.56	967.22	896.10
cryst color	Orange	red	red
cryst dimens (mm)	0.25 × 0.20 × 0.15	0.30 × 0.20 × 0.15	0.15 × 0.10 × 0.08
cryst syst	orthorhombic	triclinic	monoclinic
space group	*P*2(1)2(1)2(1)	$P\bar{1}$	*P*2(1)/*c*
unit cell dimensions			
a (Å)	7.979(3)	11.888(2)	15.177(11)
b (Å)	9.383(4)	12.474(3)	10.778(8)
c (Å)	29.536(12)	18.948(3)	26.82(2)
β (deg)	90	107.317(2)	90.859(10)
V (Å$^{3)}$	2211.1(16)	2408.3(8)	4386(6)
Z	4	2	4
D_c (g·cm^{-3})	1.612	1.332	1.357
μ (mm^{-1})	4.244	1.985	2.173
F(000)	1068	1008	1860
radiation (λ = 0.710730Å)	Mo Kα	Mo Kα	Mo Kα
temperature (K)	293(2)	293(2)	293(2)
scan type	$\phi-\omega$	$\phi-\omega$	$\phi-\omega$
θ range (deg)	2.28 to 27.00	1.82 to 25.01	1.34 to 25.01
h,k,l range	$-10 \le h \le 9$, $-11 \le k \le 11$, $-36 \le l \le 37$	$-14 \le h \le 14$, $-14 \le k \le 14$, $-22 \le l \le 10$	$-18 \le h \le 17$, $-12 \le k \le 12$, $-31 \le l \le 27$
no. of reflns measd	10 883	10 164	17 611
no. of unique reflns	4698 [R_{int} = 0.0498]	8380 [R_{int} = 0.0225]	7673 [R_{int} = 0.0569]
completeness to θ	98.9% (θ = 27.00)	98.7% (θ = 25.01)	99.4% (θ = 25.01)
max. and min. transmn	0.5685 and 0.4167	0.7550 and 0.5873	0.8453 and 0.7364
refinement method	full-matrix least-squares on F^2	full-matrix least-squares on F^2	full-matrix least-squares on F^2
no. of data/restraints/params	4698/0/253	8380/0/532	7673/0/487
goodness-of-fit on F^2	1.093	0.954	1.174
final *R* indices [$I > 2\sigma(I)$]	R_1 = 0.0316, wR_2 = 0.0706	R_1 = 0.0336, wR_2 = 0.0718	R_1 = 0.0742, wR_2 = 0.1809
R indices (all data)	R_1 = 0.0336, wR_2 = 0.0712	R_1 = 0.0440, wR_2 = 0.0744	R_1 = 0.0881, wR_2 = 0.1865
largest diff peak and hole (e·Å^{-3})	1.257 and −1.233	1.244 and −0.682	3.167 and −3.294

mmol) followed by crystallization from THF at −15 °C afforded pure **3b** as orange-red crystals. Yield: 0.483 g (69% based on Yb). Anal. Calcd for $C_{36}H_{46}N_4OYb_2$: C, 48.21; H, 5.17; N, 6.25. Found: C, 48.02; H, 5.21; N, 6.20. IR (Nujol, cm^{-1}): 3091 (m), 1063 (s), 1545 (w), 1439 (s), 1426 (s), 1390 (vs), 1350 (m), 1338 (w), 1311 (m), 1292 (m), 1261(w), 1228 (m), 1152 (w), 1119 (w), 1067 (w), 1014 (m), 937(w), 865 (w), 771 (vs).

Preparation of Cp$_2$Yb[η^1:η^2-CyNC(NHCy)NC$_6$H$_4$NH$_2$-2] (4a). To a solution of **1c** (0.706 g, 0.86 mmol) in 30 mL of THF was added *N*,*N*′-dicyclohexylcarbodiimide (0.355 g, 1.72 mmol) at −30 °C, and the resulting mixture was stirred for 2 h, then for 12 h at room temperature. The suspension was filtered, the red filtrate was concentrated (3 mL), and *n*-hexane (15 mL) was added to precipitate a red solid, which was filtered, washed with *n*-hexane (3 × 5 mL), and then dried under reduced pressure to obtain **4a** (0.684 g, 65%) as a red powder. Anal. Calcd for $C_{29}H_{35}YbN_4$: C, 56.85; H, 5.76; N, 9.14. Found: C, 56.78; H, 5.72; N, 9.08. IR (Nujol, cm^{-1}): 3359 (m), 3308 (s), 3268 (s), 3080 (w), 3021 (w), 1643 (w), 1623 (m), 1538 (vs), 1490 (vs), 1437 (vs), 1321 (m), 1311 (s), 1273 (s), 1172 (s), 1128 (m), 1020 (s), 859 (w), 773 (vs), 739 (s), 645 (m).

Preparation of Cp$_2$Yb[η^1:η^2-^{i}PrNC(NH^{i}Pr)NC$_6$H$_4$NH$_2$-2] (4b). Following the procedure described for **4a**, using **1c** (0.591 g, 0.72 mmol) and *N*,*N*′-diisopropylcarbodiimide (0.182 g, 1.44 mmol), **4b** was obtained as a red powder (0.379 g, 49%). Recrystallization of **4b** from THF at −15 °C afforded orange crystals suitable for X-ray analysis. Anal. Calcd for $C_{23}H_{31}YbN_4$: C, 51.49; H, 5.82; N, 10.44. Found: C, 51.32; H, 5.79; N, 10.38. IR (Nujol, cm^{-1}): 3368 (m), 3321 (s), 3269 (s), 3087 (w), 3030 (w), 1627 (w), 1612 (m), 1549 (vs), 1492 (vs), 1432 (vs), 1331 (m), 1310 (s), 1269 (s), 1172 (s), 1128 (m), 1112 (m), 1020 (s), 909 (w), 854 (w), 771 (vs), 739 (s), 641 (m).

Preparation of Cp$_2$Yb[η^1:η^2-CyNC(NHCy)NC$_6$H$_4${NC(NHCy)$_2$-2}] (5a). Method A. To a solution of **4a** (0.342 g, 0.56 mmol) in 30 mL of THF was added *N*,*N*′-dicyclohexylcarbodiimide (0.115 g, 0.56 mmol) at −30 °C, and the resulting mixture was stirred for 12 h at room temperature. The red solution was concentrated and *n*-hexane layered to give **5a**·2THF as red crystals. Yield: 0.314 g (58%). Anal. Calcd for $C_{50}H_{76}N_6O_2Yb$: C, 62.15; H, 7.93; N, 8.70. Found: C, 62.01; H, 7.88; N, 8.66. IR (Nujol, cm^{-1}): 3419(m), 3329 (s), 3086 (w), 3050 (w), 1628 (w), 1578 (s), 1550 (vs), 1498 (vs), 1421 (s), 1390 (m), 1344 (w), 1305 (m), 1291 (s), 1263 (s), 1238 (m), 1190 (m), 1147 (m), 1095 (m), 1059 (s), 1015 (m), 977 (w), 945 (w), 893 (m).842 (w), 765 (vs).

Method B. To a solution of **1c** (0.443 g, 0.54 mmol) in 30 mL of THF was added *N*,*N*′-dicyclohexylcarbodiimide (0.446 g, 2.16 mmol) at −30 °C, and the resulting mixture was stirred for 12 h at room temperature. The red solution was concentrated and *n*-hexane layered to give red crystals of **5a**·2THF (0.678 g, 65%).

Preparation of Cp$_2$Yb[η^1:η^2-^{i}PrNC(NH^{i}Pr)NC$_6$H$_4${NC(NH^{i}Pr)$_2$-2}] (5b). Following the procedure described for **5a**, method A. Reaction of **4b** (0.189 g, 0.35 mmol) with 1 equiv of *N*,*N*′-diisopropylcarbodiimide (0.442 g, 0.35 mmol) gave **5b**·2THF as a red solid at −15 °C. Yield: 0.189 g (61%). Anal. Calcd for $C_{44}H_{68}N_6O_2Yb$: C, 59.64; H, 7.73; N, 9.48. Found: C, 59.57; H, 7.68; N, 9.45. IR (Nujol, cm^{-1}): 3401 (m), 3257 (s), 3068 (m), 1621 (m), 1587 (s), 1490 (s), 1324 (m), 1298 (s), 1219 (w), 1155 (m), 1117 (m), 1075 (m), 1009 (m), 970 (m), 922 (s), 891 (m), 752 (vs), 665 (s).

Method B. To a solution of **1c** (0.540 g, 0.62 mmol) in 30 mL of THF was added *N*,*N*′-diisopropylcarbodiimide (0.313 g, 2.48 mmol) at −30 °C, and the resulting mixture was stirred for 12 h at room temperature. The red solution was concentrated and *n*-hexane layered to give red crystals of **5b**·2THF (0.670 g, 61%).

Preparation of Cp$_2$Yb[η^1:η^2-CyNC(NHCy)NC$_5$H$_3$N{NC(NHCy)$_2$-3}] (6). To a solution of **1d** (0.397 g, 0.48 mmol) in 30 mL of THF was added *N*,*N*′-dicyclohexylcarbodiimide (0.396 g, 1.92 mmol) at −30 °C. After stirring for 2 h at low temperature, the reaction solution was slowly warmed to room temperature and stirred for another 12 h. The red solution was concentrated to give red crystals of **6**·THF (0.542 g, 63%). Anal. Calcd for $C_{45}H_{68}N_7OYb$: C, 60.31; H, 7.65; N, 10.94. Found: C, 60.23; H, 7.59; N,

Table 4. Crystal and Data Collection Parameters of Complexes 7, 8a, and 8b

	7·1.5THF	**8a**	**8b**
formula	$C_{57}H_{81}N_7O_{1.5}Yb_2$	$C_{30}H_{41}N_4Yb$	$C_{24}H_{32}N_4Yb$
molecular weight	1234.37	630.71	274.79
cryst color	red	red	red
cryst dimens (mm)	0.20 × 0.15 × 0.15	0.20 × 0.10 × 0.10	0.15 × 0.10 × 0.10
cryst syst	triclinic	orthorhombic	orthorhombic
space group	$P\bar{1}$	*Pccn*	*P*2(1)2(1)2(1)
unit cell dimensions			
a (Å)	12.774(4)	16.007(5)	8.357(2)
b (Å)	13.259(4)	32.816(9)	9.922(3)
c (Å)	17.183(6)	10.753(3)	28.681(8)
β (deg)	72.551(4)	90	90
V (Å$^{3)}$	2697.3(15)	5649(3)	2378.4(12)
Z	2	8	8
D_c (g·cm^{-3})	1.520	1.483	1.535
μ (mm^{-1})	3.492	3.335	3.948
F(000)	1284	2552	1096
radiation (λ = 0.710730 Å)	Mo Kα	Mo Kα	Mo Kα
temperature (K)	293(2)	293(2)	293(2)
scan type	$\omega-2\theta$	$\omega-2\theta$	$\omega-2\theta$
θ range (deg)	1.58 to 26.01	1.24 to 26.01	1.42 to 26.00
h,*k*,*l* range	$-13 \le h \le 15$, $-16 \le k \le 16$, $-17 \le l \le 21$	$19 \le h \le 19$, $-30 \le k \le 40$, $-12 \le l \le 13$	$-10 \le h \le 10$, $-11 \le k \le 12$, $-35 \le l \le 27$
no. of reflns measd	12 433	24 643	10 921
no. of unique reflns	10 382 [R_{int} = 0.0278]	5556 [R_{int} = 0.0383]	4652 [R_{int} = 0.0272]
completeness to θ	97.8% (θ = 26.01)	99.9% (θ = 26.01)	99.8% (θ = 26.00)
max. and min. transmn	0.6224 and 0.5418	0.7315 and 0.5551	0.6936 and 0.5889
refinement method	full-matrix least-squares on F^2	full-matrix least-squares on F^2	full-matrix least-squares on F^2
no. of data/restraints/params	10 382/6/598	5556/0/316	4652/0/262
goodness-of-fit on F^2	1.013	1.098	0.960
final *R* indices [$I > 2\sigma(I)$]	R_1 = 0.0410, wR_2 = 0.1115	R_1 = 0.0311, wR_2 = 0.0710	R_1 = 0.0252, wR_2 = 0.0424
R indices (all data)	R_1 = 0.0628, wR_2 = 0.1245	R_1 = 0.0495, wR_2 = 0.0768	R_1 = 0.0289, wR_2 = 0.0431
largest diff peak and hole (e·Å^{-3})	1.701 and −1.244	1.541 and −0.550	0.637 and −0.671

10.88. IR (Nujol, cm^{-1}): 3405 (m), 3318 (s), 3270 (m), 3082 (w), 1572 (vs), 1526 (s), 1346 (s), 1285 (m), 1261 (s), 1206 (m), 1150 (m), 1099 (m), 1070 (m), 1017 (s), 980 (w), 889 (m), 842 (w), 763 (vs).

Preparation of (Cp$_2$Yb)$_2$[η^2:η^3-(NCy)$_2$CNC$_5$H$_3$N{NC(NHCy)$_2$-3}] (7). A solution of **6** (0.50 mmol) in 30 mL of THF was heated to reflux for 5 h, then cooled to room temperature and concentrated. After 1 week, the red crystals of **7**·1.5THF (0.13 g, 42% based on Yb) were separated from the mother liquor by filtration. Anal. Calcd for $C_{57}H_{81}N_7O_{1.5}Yb_2$: C, 55.46; H, 6.61; N, 7.94. Found: C, 55.41; H, 6.55; N, 7.89. IR (Nujol, cm^{-1}): 3500 (m), 3380 (s), 3330 (m), 3082 (w), 1610 (m), 1575 (vs), 1520 (s), 1330 (s), 1285 (m), 1251 (s), 1200 (m), 1130 (m), 1070 (m), 1054 (m), 1015 (s), 980 (w), 885 (m), 842(w), 761 (vs).

Preparation of Cp$_2$Yb[η^2:η^1-CyNC(NHCy)NC$_6$H$_4$(CH$_2$NH$_2$-2)] (8a). Following the procedure described for **4b**, reaction of **1e** (0.543 g, 1.28 mmol) with 1 equiv of *N*,*N*′-dicyclohexylcarbodiimide (0.264 g, 1.28 mmol) gave **8a** as red crystals. Yield: 0.67 g (83%). Anal. Calcd for $C_{30}H_{41}N_4Yb$: C, 57.13; H, 6.55; N, 8.88. Found: C, 56.91; H, 6.51; N, 8.85. IR (Nujol, cm^{-1}): 3393 (w), 3335 (w), 3282 (w), 3070 (w), 3025 (w), 1598 (m), 1577 (s), 1552 (vs), 1485 (vs), 1418 (m), 1368 (m), 1344 (w), 1305 (m), 1290 (m), 1259 (m), 1240 (w), 1150 (w), 1075 (m), 1011 (m), 977 (w), 927 (w), 890 (m), 778 (s), 707 (w).

Preparation of Cp$_2$Yb[η^2:η^1-^{i}PrNC(NH^{i}Pr)NC$_6$H$_4$(CH$_2$NH$_2$-2)] (8b). Following the procedure described for **4b**, reaction of **1e** (0.662 g, 1.56 mmol) with *N*,*N*′-diisopropylcarbodiimide (0.197 g, 1.56 mmol) gave **8b** as red crystals. Yield: 0.669 g (78%). Anal. Calcd for $C_{24}H_{32}N_4Yb$: C, 52.45; H, 5.87; N, 10.19. Found: C, 52.28; H, 5.83; N, 9.13. IR (Nujol, cm^{-1}): 3411 (w), 3334 (m), 3257 (s), 3061 (w), 3054 (w), 1573 (s), 1551 (vs), 1486 (vs), 1417 (s), 1380 (s), 1356 (m), 1303 (vs), 1273 (w), 1204 (w), 1170 (m), 1126 (w), 1080 (m), 1011 (m), 976 (w), 937 (w), 921 (w), 773 (s), 746 (m).

Crystal Structure Determination. Suitable single crystals were sealed under N_2 in thin-walled glass capillaries. X-ray diffraction data were collected on a SMART APEX CCD diffractometer (graphite-monochromated Mo Kα radiation, $\phi-\omega$ scan technique, λ = 0.71073 Å). The intensity data were integrated by means of the SAINT program.[41] SADABS[42] was used to perform area-detector scaling and absorption corrections. The structures were solved by direct methods and were refined against F^2 using all reflections with the aid of the SHELXTL package.[43] All non-hydrogen atoms were refined anisotropically. The H atoms were included in calculated positions with isotropic thermal parameters related to those of the supporting carbon atoms but were not included in the refinement. All non-hydrogen atoms were found from the difference Fourier syntheses. All calculations were performed using the Bruker Smart program. There are two heavily disordered Cp rings present per formula unit for **1b**, which have been modeled. Crystallographic parameters for compounds **1a**−**e**, **2a**, **3a**, **4b**, **5a**·2THF, **6**·THF, **7**·1.5THF, **8a**, and **8b**, along with details of the data collection and refinement, are collected in Tables 1−4. Selected bond distances and angles for each are given in Figures 1−13, respectively. Further details are included in the Supporting Information.

Acknowledgment. We thank the NNSF of China and NSF of Shanghai for financial support.

Supporting Information Available: Tables of atomic coordinates and thermal parameters, all bond distances and angles, and experimental data for all structurally characterized complexes. This material is available free of charge via the Internet at http://pubs.acs.org.

OM061094+

(41) *SAINTPlus Data Reduction and Correction Program* v. 6.02 a; Bruker AXS: Madison, WI, 2000.

(42) Sheldrick, G. M. *SADABS*, A Program for Empirical Absorption Correction; University of Göttingen: Göttingen, Germany, 1998.

(43) Sheldrick, G. M. *SHELXL-97*, Program for the Refinement of Crystal Structures; University of Göttingen: Göttingen, Germany, 1997.